

Czech University of Life Sciences Prague

Faculty of Agrobiolgy, Food and Natural Resources

**Department of Agroenvironmental Chemistry and Plant
Nutrition**



**Czech University
of Life Sciences Prague**

**Uptake of Per- and Polyfluoroalkyl Substances (PFAS) by
Plants**

Master's thesis

**Bc. Saša Žůrková
Waste Technology**

Supervisor: Ing. Filip Mercl, Ph.D.

© 2024 CZU in Prague

Declaration

I hereby declare that I have authored this master's thesis carrying the name „Uptake of Per- and Polyfluoroalkyl substances (PFAS) by Plants “independently under the guidance of my supervisor. Furthermore, I confirm that I have used only professional literature and other information sources that have been indicated in the thesis and listed in the bibliography at the end of the thesis. As the author of the master's thesis, I further state that I have not infringed the copyrights of third parties in connection with its creation.

In Prague on the 19th of April 2024

Acknowledgments

I would like to thank my supervisor, Ing. Filip Mercl, Ph.D., for his help and valuable advice in writing my thesis. I would also like to thank my family and friends for their support during my studies. Many thanks also go to Bc. Markéta Mičudová, with whom we collaborated on the pot experiment and who was always willing to help me.

Uptake of Per- and Polyfluoroalkyl substances (PFAS) by Plants

Summary:

Currently, more and more attention is paid to a group of chemicals called per- and polyfluorinated substances (PFAS). These substances include a wide variety of synthetic compounds that are widely used in industry due to their exceptional properties. However, their extensive use and resistance to degradation have led to their widespread presence in the environment. PFAS have been found in soil, water, or air. Through contaminated water and soil, PFAS have penetrated plant roots to the fruits or seeds of cultivated crops, where they become part of the food chain. This contamination poses a potential health risk to the human population and ecosystems. Concerns about the toxicity and persistence of PFAS have recently led to efforts to prevent PFAS from contaminating the food chain. Therefore, some representatives of the PFAS group are gradually being restricted. It is an effort to prevent PFAS, which have already entered the environment, from escaping into water and subsequently into plants. The use of biochar, which can sorb contaminants on its surface and also improve soil properties, may potentially be suitable for PFAS sorption in soil. At the same time, it is also possible to use waste materials (wood, sewage sludge, agricultural residues, food waste) to produce biochar, which represents a sustainable cycle of dealing with these materials.

In this work, the effect of biochar on the uptake of PFAS by *Cucurbita pepo* L., a variety of zucchini, was investigated in the pot experiment. The presence or absence of biochar made from sewage sludge or wood was chosen as a factor. The plants were irrigated with 5 representatives of PFAS, namely HFPO-DA, HFPO-TA, HFPO-TeA, PFOA, and PFOS, at a concentration of 10 µg/L for 41 days. The chosen concentration of PFAS in the irrigation water was consulted with the scientific literature. A total of 78.15 µg of each contaminant was added to each plant. Subsequently, the amount of contaminants that got into the fruits was evaluated, and their potential risk when consumed by an adult and a child was estimated.

No statistically significant difference was observed between the amount of contaminants in fruits grown on variants with and without biochar. Contaminants were found in the fruits of plants grown on all variants treated with the PFAS solution. HFPO-DA was the most detected in fruits across the variants, followed by PFOA and PFOS. Contaminants HFPO-TeA and HFPO-TA were the least detected in fruits. The reason for the different uptake of contaminants by plants could be the different molecular weights and structure of the contaminants.

The risk for an adult would be the consumption of 352 ng of PFAS per week, for a child the risk would be the consumption of 88 ng of PFAS per week. This risk dose would be reached by consuming 143 to 306 g of zucchini, depending on the variant. This represents a real consumable dose during the week, as 300 grams is the average weight of a zucchini fruit. For a child, the risk dose would be reached by consuming 36 to 77 g of zucchini, depending on the variant, which again represents a realistic dose that a child could consume in a week.

Keywords: PFOA, PFOS, accumulation, zucchini, biochar

Content

1	Introduction	1
2	Scientific hypothesis and aims of the thesis	2
3	Literature research	3
3.1	PFAS Distribution	3
3.1.1	Polymeric PFAS	4
3.1.1.1	Fluoropolymers	4
3.1.1.2	Polymeric perfluoropolyethers	4
3.1.1.3	Side-chain fluorinated polymers	5
3.1.2	Non-polymers PFAS	5
3.1.2.1	Perfluoroalkyl substances	6
3.1.2.2	Polyfluoroalkyl substances	10
3.2	Structure of commonly known PFAS	10
3.2.1	Carbon – fluorine tail	10
3.2.2	Functional group	11
3.3	Use of PFAS in industry	12
3.4	PFAS entrances into the environment	13
3.5	PFAS in soils	14
3.5.1	PFAS sorption in soil	15
3.5.1.1	Sorption on the organic part of the soil	16
3.5.1.2	Sorption on mineral part of soil	16
3.5.2	Properties of PFAS affecting soil sorption	17
3.6	PFAS in plants	18
3.6.1	PFAS in root	18
3.6.2	PFAS in aboveground biomass of plant	19
3.6.3	What affects the uptake and movement of PFAS in plants?	20
3.6.3.1	Abiotic factors	20
3.6.3.2	Plant	21
3.6.3.3	PFAS molecule	21
3.7	Biochar as PFAS remediation agent	22
3.7.1	Production of biochar	22
3.7.2	Pyrolysis process	23
3.7.3	Biochar from Sewage Sludge in relation to PFAS	24
3.7.4	Biochar from timber waste as a sorbent of PFAS	25
3.8	PFAS in the human organism	26
3.9	Limits of PFAS in the environment	27
4	Methodology	28

4.1	Preparation of an outdoor experiment.....	29
4.2	Irrigation.....	30
4.3	Preparation of chemicals	31
4.3.1	Preparation of the stock solution	31
4.3.2	Preparation of the irrigation solution	31
4.4	Harvest	31
4.5	Laboratory part of the experiment.....	34
4.6	Statistical data processing	37
5	Results.....	38
5.1	Yield of fresh and dried fruit biomass.....	38
5.2	The effect of biochar on the amount of PFAS in fruits.....	39
5.3	The relationship between the weight of zucchini and the total amount of contaminants.....	43
5.4	Distribution factor.....	47
6	Discussion	48
6.1	Environmental relevance of PFAS concentration in water.....	48
6.2	Effect of biochar and PFAS on fruit weight	49
6.2.1	Effect of biochar on fruit weight.....	49
6.2.2	Effect of PFAS on fruit weight	50
6.3	Effect of biochar on PFAS uptake	51
6.3.1	Uptake of PFAS by plants	51
6.3.2	Effect of biochar on PFAS uptake	52
6.4	The riskiness of fruits when consumed	52
6.4.1	Riskiness of fruits for adults	52
6.4.2	Riskiness of fruits for children.....	54
7	Conclusion	56
8	Bibliography	57
9	Appendices.....	I
9.1	Appendix 1 – Weight of zucchini fruits.....	I
9.2	Appendix 2 – Concentrations of contaminants measured in individual plants II	II
9.3	Appendix 3 – Amount of contaminants measured in individual plants....	III
9.4	Appendix 4 – Uptake of contaminants from individual plants.....	III

1 Introduction

PFAS is the abbreviated name for a group of substances known as per and polyfluorinated compounds. This broad group of man-made substances contains over 12,000 compounds (Wallace et al. 2023). Due to their unique properties, these substances are used in industry to produce non-stick coatings, materials that repel water, grease, and oil, and firefighting foams (Agency for Toxic Substances and Disease Registry 2022). The most well-known compounds that fall into the PFAS group are perfluorooctanoic acid (PFOA) and perfluorooctanesulfonic acid (PFOS) (Lesmeister et al. 2021).

PFAS are substances that have contaminated the entire environment in recent decades. PFAS have been found in soils on every continent, surface, and groundwater, and even in animals, including humans (Ghisi et al. 2019; Sørmo et al. 2021; Krahn et al. 2023). Due to the mobility of PFAS and their tendency to accumulate in the environment, their use is now restricted in Europe. Two compounds from the PFAS group have already been classified as persistent organic pollutants (POPs) by the Stockholm Convention. Specifically, PFOA and PFOS, have been the most widely used in the past (Krahn et al. 2023). PFOA production is restricted under the Stockholm Convention, while PFOS production is already banned (Munoz et al. 2019; Gui et al. 2023; Sun et al. 2023). In 2022, perfluorohexanesulphonic acid (PFHxS) was also approved for inclusion in the list of persistent organic pollutants (MŽP 2023).

Soil is an important reservoir of persistent PFAS. These compounds enter the soil through contaminated irrigation water, wet or dry atmospheric deposition, or the application of contaminated sludge to the soil. PFAS may subsequently sorb to soil particles or dissolve into the soil solution. From there, they can enter plants and contaminate the food chain up to humans (Mei et al. 2021). According to EPA (2023a), many PFAS have already been detected in the blood of both animals and humans. In humans, PFAS can cause several pathological changes, including cancer (Ghisi et al. 2019).

Preventing or limiting the movement of water-soluble PFAS in the soil-plant system would be possible with appropriate remediation techniques, according to Sørmo et al. (2021). For this purpose, carbon-based sorbents have been investigated in the last few decades. These can strongly bind organic contaminants. This prevents their leaching into water and subsequent bioaccumulation of PFAS in plants. Carbon-based sorbents include biochar, which was used in this thesis.

The banned PFOA and PFOS have been gradually replaced by other compounds from the PFAS group in the industry (Reade 2018). The most commonly used PFOA has been replaced by hexafluoropropylene oxide dimer acid and its ammonium salt (commercial name GenX) and PFOS has been replaced by perfluorobutane sulfonic acid (PFBS) and its potassium salt (Xu et al. 2021; EPA 2023b). These shorter-chain PFAS were considered less persistent in the environment. However, GenX has been shown to be more toxic than PFOA. At the same time, substitutes are equally or more persistent than banned PFAS (Xu et al. 2021). Therefore, these compounds have been termed as regrettable substitution ('regrettable substitution') by Reade (2018). Other PFAS substitutes include 6:2 chlorinated polyfluoroalkyl ether sulfonate (F-53B) and sodium p-perfluorooctanoic nonenoxybenzene sulfonate (OBS). However, these are not as safe as expected (Xu et al. 2021).

2 Scientific hypothesis and aims of the thesis

The hypothesis of the thesis: The application of biochar into the soil will reduce PFAS uptake by plants.

Objective of thesis: To assess the effect of biochar amendment of soil on the uptake and accumulation of selected PFAS from irrigation water by plants.

3 Literature research

3.1 PFAS Distribution

PFAS are a group of synthetic prepared amphiphilic organic molecules. These molecules comprise a strong hydrophobic carbon-fluorine tail and a hydrophobic functional group (Mei et al. 2021). These two molecule parts give PFAS their specific properties and determine their persistence in the environment and their reactivity (Ghisi et al. 2019).

OECD (2021) defines PFAS as a fluorinated substance where a perfluorinated methyl group (-CF₃) or perfluorinated methylene group (-CF₂-) can be found. At least one carbon atom is fully fluorinated in PFAS, so there are no chlorine, bromine, hydrogen, or iodide atoms attached to the carbon atom.

PFAS are a broad group of compounds containing linear or branched (Ghisi et al. 2019; Ramírez Carneo et al. 2021) molecules with very different physical and chemical properties. Differences can be observed in molecular size, charge, state of matter, volatility, mobility, or bioaccumulation (Cousins et al. 2020). Based on the differences in properties, the family of PFAS has been divided into two classes, which are then further subdivided into subclasses, groups, and subgroups (ITRC 2023). A schematic of the division of PFAS can be found in Figure 1.

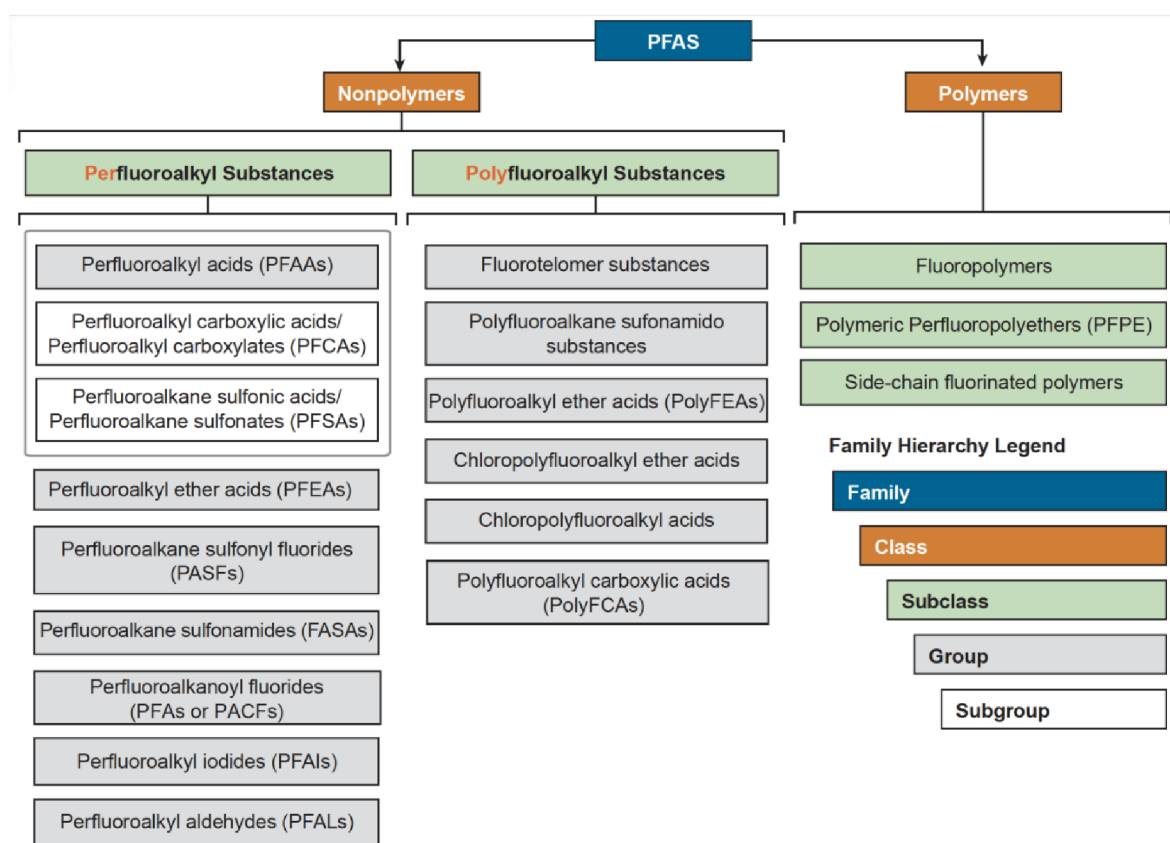


Figure 1: The PFAS's family tree (ITRC 2023).

The next chapters will describe two basic classes (polymers and non-polymers).

3.1.1 Polymeric PFAS

Polymers are huge molecules that consist of monomers. Monomers are many shorter chain molecules with no repeating units (ITRC 2023). Due to the size of the molecule, polymers have different physical, chemical, and biological properties compared to non-polymers with lower molecular weight (Henry et al. 2018). There are three subclasses within this class:

- Fluoropolymers
- Polymeric perfluoropolyethers (PFPE)
- Side-chain fluorinated polymers (SCFP) (ITRC 2023; Lohmann & Letcher 2023).

3.1.1.1 Fluoropolymers

Fluoropolymers are high molecular-weight polymers (molecular weight well over 100,000 Da) (Henry et al. 2018) that consist of a carbon-only polymer backbone to which fluorine atoms are directly attached (ITRC 2023). These are mostly extremely stable substances that are not subject to thermal, chemical, photochemical, hydrolytic, oxidative, or biological degradation (Henry et al 2018). Fluoropolymers are virtually insoluble in water, meaning that they do not move long distances and are difficult for organisms to access (Lohmann & Letcher 2023). The main representatives of fluoropolymers are:

- Polytetrafluoroethylene (PTEE)
- Ethylene tetrafluoroethylene (ETFE)
- Copolymer Fluorinated ethylene propylene (FEP)
- Perfluoroalkoxy alkanes (PFA)


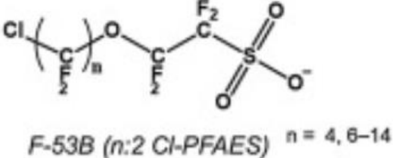
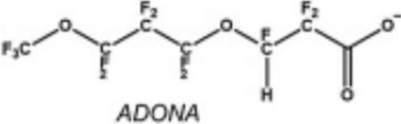
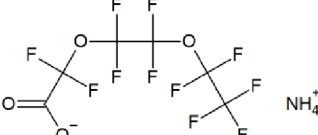
In some cases, non-polymeric substances are used as processing aids in the production of fluoropolymers. These, together with unreacted monomers, may then be released into the environment from the resulting fluoropolymers (ITRC 2023).

3.1.1.2 Polymeric perfluoropolyethers

Polymeric perfluoropolyethers are also known as ether-PFAS (Lohmann & Letcher 2023). These compounds have fluorine atoms bonded to carbon atoms found in the carbon and oxygen polymer backbone. An ether bond (C-O-C) is found between carbon and oxygen atoms in the backbone (Munoz et al. 2019; ITRC 2023; Lohmann & Letcher 2023). These polymeric compounds have not yet been closely characterized in the environment (ITRC 2023).

These compounds are considered to replace PFOA and PFOS, which have long chain lengths. The ether-PFAS group includes the carboxylic compounds the ammonium salt of hexafluoropropylene oxide dimer acid (GenX), Difluoro[1,1,2,2-tetrafluoro-2-(pentafluoroethoxy)] ethoxy acetic acid (EEA-NH₄) (Munoz et al. 2019; Lohmann & Letcher 2023) as well as the sulfonated compound 6:2 chlorinated polyfluoroalkyl ether sulfonate (F-53B). Another ether-PFAS representative that contains a carboxyl group is the ammonium salts of dodecafluoro-3H-4,8-dioxananoate (ADONA) (Munoz et al. 2020; Lohmann & Letcher 2023). However, this substance is identified by ITRC (2023) as the most important representative of polyfluoroalkyl substances. The structural formulas of the listed representatives of polymeric perfluoropolyethers are shown in Table 1.

Table 1: The structural formulas of GenX (Brandsma et al. 2019), F-53B, ADONA (Munoz et al. 2019), and EEA-NH4 (Environmental Agency 2023).

Compound	Structural formula
GenX	
F-53B	
ADONA	
EEA-NH4	

3.1.1.3 Side-chain fluorinated polymers

The name side-chain fluorinated polymers (SCFP) is derived from the structure of these compounds. The molecule consists of a nonfluorinated polymer backbone on which fluorinated side chains are attached (ITRC 2023). In some cases, the fluorinated side chain may be released (e.g. by hydrolysis of the ester linkage) from the molecule to form perfluoroalkyl acids and a fluorinated monomer residue (CLU-IN 2023; Lohmann & Letcher 2023). Side-chain fluorinated polymers are therefore referred to as precursors of PFAA formation. This subgroup of polymers includes:

- Fluorinated urethane polymers
- Fluorinated acrylate/methacrylate polymers
- Fluorinated oxetane polymers (ITRC 2023)

Although fluoropolymers are referred to as "polymers of low concern" in the literature, they have already been found in the environment. SCFP, from whose molecules short non-polymeric fluorinated chains can be released, also appears to be problematic (Lohmann & Letcher 2023).

3.1.2 Non-polymers PFAS

Non-polymeric PFAS are much more frequently mentioned in environmental studies compared to polymeric PFAS (Lohmann & Letcher 2023). This is because non-polymeric

PFAS are the most commonly detected in the environment, including humans (ITRC 2023). The scientific work most often focuses on:

- perfluorooctanoic acid (PFOA)
- perfluorooctane sulfonic acid (PFOS)
- perfluorohexane sulfonic acid (PFHxS)
- perfluorononanoic acid (PFNA).

Based on the description of these 4 PFAS, the biological impact of the whole group of PFAS is assessed, as the other compounds are not well described (Cousins et al. 2020).

Non-polymeric PFAS can be divided into two subclasses, which are further subdivided into different numbers of groups and subgroups. The first subclass is perfluoroalkyl substances, which have a fully fluorinated alkyl group (Ramírez Carneo et al. 2021; CLU-IN 2023). The second subclass is polyfluoroalkyl substances with not all hydrogen atoms substituted by atoms of fluorine (Buck et al. 2011; CLU-IN 2023).

The division of non-polymeric PFAS is not entirely clear; the authors omit some examples in their schemes or use different terms when dividing PFAS. The differences are evident, for example, when comparing the sources of ITRC et al. (2023) and Henry et al. (2018). Henry et al. (2018) name the PFAS family as a group, the class of non-polymeric and polymeric compounds as a category, and the subclasses of perfluoroalkyl and polyfluoroalkyl substances carry the class designation in the article. These subsections will be based on the distribution published by the ITRC (2023).

3.1.2.1 Perfluoroalkyl substances

Perfluoroalkyl substances are a group of substances with a specific structure. These molecules typically contain 4 to 16 carbon atoms (Ghisi et al. 2019; Ramírez Carneo et al. 2021). In a perfluoroalkyl compound molecule, all hydrogen atoms are replaced by a fluorine atom (Ghisi et al. 2019). Furthermore, a functional group is present in the molecule. In that, the hydrogen atoms are never replaced by fluorine because this would change the nature of the functional group (Ramírez Carneo et al. 2021).

The most common substances encountered are those containing a carboxyl or sulfonic functional group, but there may be others (ITRC 2023). Thus, the general structure of the molecule can be described as $C_nF_{2n+1}-R$, where C_nF_{2n+1} represents the length of the C-F chain ($n > 2$) and R is the functional group at the end of the molecule (Mei et al. 2021; ITRC 2023).

This subclass includes the groups:

Subgroups belonging to this group are (ITRC 2023):

- perfluoroalkyl acids (PFAA)
- perfluoroalkyl ether acids (PFEA)
- perfluoroalkane sulfonyl fluorides (PASF)
- perfluoroalkane sulfonamides (PFASA)
- perfluoroalkanoyl fluorides (PFA/PACF)
- perfluoroalkyl iodides (PFAI)
- perfluoroalkyl aldehydes (PFAL)

3.1.2.1.1 Perfluoroalkyl acids (PFAA)

PFAA is considered the most prevalent environmental contaminant from PFAS (Ghisi et al. 2019). Of the PFAS group (family, according to this division), the structure of PFAA is considered less complex. Nevertheless, these compounds are virtually indegradable in the environment. Due to biotic and abiotic conditions, some more complex polyfluoroalkyl substances decompose on PFAA (ITRC 2023).

The PFAA group can be divided into several subgroups. According to ITRC (2023), the best-known subgroups are:

- perfluoroalkyl carboxylic acids (PFCA)
- perfluoroalkane sulfonic acids (PFSA)

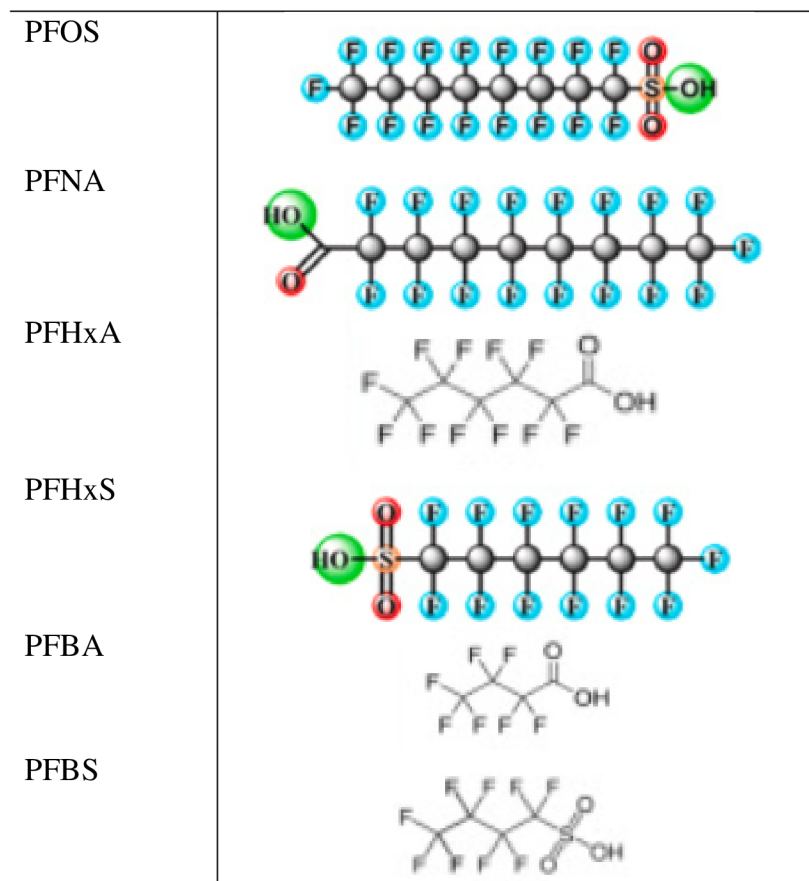
PFCA containing a carboxylic functional group (-COOH) have a molecular formula of $C_{n-1}F_{2n-1}COOH$. The sum formula of PFSA containing a sulfonic functional group (-SO₃H) is $C_nF_{2n+1}-SO_3H$ (Mei et al. 2021; Leung et al. 2023). Compounds from both subgroups, i.e., PFCA and PFSA, can be released during the decomposition of more complex PFAS compounds. Examples include the formation of PFCA representatives from fluorotelomer alcohols (FTOH) or the formation of PFSA representatives from perfluoroalkane sulfonamide ethanols (FASE) (ITRC 2023).

The most well-known representative of the PFCA subgroup is PFOA, and of the PFSA subgroup, the most well-known representative is PFOS. These substances are known mainly because they have been widely industrially produced in the past and subsequently scientifically investigated (Ghisi et al. 2019; Semerád et al. 2020). Both of these substances are banned (Reade 2018) and are also considered among the most abundant organic pollutants detected in the environment, including humans (Ghisi et al. 2019). Other representatives belonging to the PFCA and PFSA groups are perfluorobutanoic acid (PFBA) perfluorohexanoic acid (PFHxA) and perfluorobutane sulfonic acid (PFBS). These short acids (PFBA and PFBS are even referred to as ultrashort by Semerád et al. (2020) are sometimes used as substitutes for the banned PFAS (Ghisi et al. 2019; Cousins et al. 2020; Kancharla et al. 2022). The best-known representatives belonging to the PFAA group are shown in Table 2.

In addition to the well-known PFCA and PFSA, the PFAA group also includes the subgroups perfluoroalkane sulfinic acids (PFSiA), perfluoroalkyl phosphonic acids (PFPA), and phosphinic acids (PFPiA), perfluoroalkyl dicarboxylic acids (PFdiCA) or perfluoroalkane disulfonic acids (PFdiSA). Some of the compounds falling into these subgroups are starting to be detected in the environment, which is drawing attention to these substances (ITRC 2023).

Table 2: The structural formulas of PFOA, PFOS, PFHxS, PFNA (Xu et al. 2021), PFBA, PFBS, PFHxA (Liu et al. 2020).

Compound	Structural formula
PFOA	



3.1.2.1.2 Perfluoroalkane Sulfonamides (PFASA)

Perfluoroalkane sulfonamides, abbreviated PFASA, sometimes referred to as FASA (Huang et al. 2019; CLU-IN 2023), are an equally important group of substances falling under PFAS (Huang et al. 2019). They are formed as products or intermediates during the electrochemical fluorination process (ITRC 2023). The use of these substances in industry leads to their proliferation in the environment. PFASA was detected in all types of water. In tap water, in wastewater, and even in natural resources. Based on the investigation of these substances, it has been found that they have negative effects not only on the environment but also on humans. The determination of these substances in the environment requires the use of more sensitive analytical methods compared to the determination of PFAA (Huang et al. 2019). These compounds are precursors to the formation of PFOS in the environment (ITRC 2023).

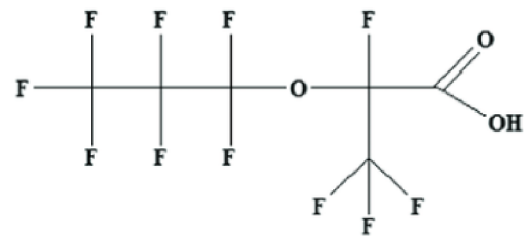
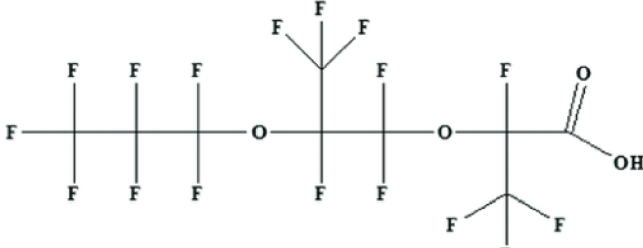
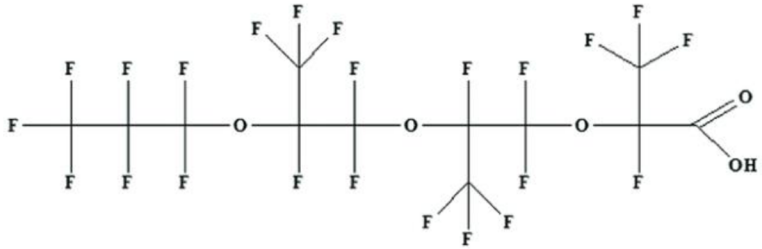
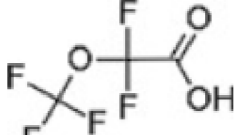
3.1.2.1.3 Other groups in the Perfluoroalkyl substances subclass

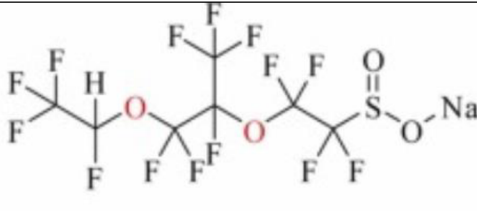
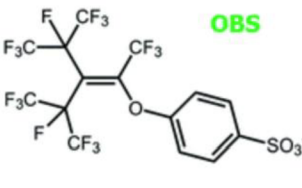
Among the other groups, PFEA are gaining in importance, which are further subdivided into the subgroups perfluoroalkyl ether carboxylic acids (PFECA) and perfluoroalkyl ether sulfonic acids (PFESA) (ITRC 2023). Substances belonging to the PFEA group contain an ether linkage in their carbon chain, as do polymeric perfluoropolyethers. This ether bond can affect the bioaccumulation of the entire ether-PFAS molecule (Munoz et al. 2019). PFECA representatives include hexafluoropropylene oxide dimer acid (HFPO-DA), hexafluoropropylene oxide trimer acid (HFPO-TA), hexafluoropropylene oxide tetramer acid (HFPO-TeA), or perfluoro-2-methoxyacetic acid (PFMOAA) (Conley et al. 2019; CLU-IN

2023; Dong et al. 2023; Sun et al. 2023). Other representatives of PFEA are 7-hydro-perfluoro-4-methyl-3,6-dioxoacetate sulfonic acid, also known as Nafion by-product 2 (Nafion BP2) (Gui et al. 2023) and Sodium p-perfluorooctane sulfonate, also known as OBS (Zhou et al. 2022). Nafion BP2 and OBS are classified as PFESA based on the sulfonic functional group (Gui et al. 2023). These substances are now used as replacements for banned PFOA and PFOS (Conley et al. 2019; Gui et al. 2023). The structural formulas of the named representatives of perfluoroalkyl substances are shown in Table 3.

Other groups falling into the perfluoroalkyl class of substances are perfluoroalkane sulfonyl fluorides (specifically perfluorooctane sulfonyl fluoride (POSF) and perfluorobutane sulfonyl fluoride (PBSF)), perfluoroalkyl iodides (PFAI), and perfluoroalkyl aldehydes (PFAL). Substances belonging to these groups are released in the production of fluorotelomer substances and polyfluorinated compounds (ITRC 2023).

Table 3: The structural formulas of HFPO-DA, HFPO-TA, HFPO-TeA (Xin et al. 2019), PFMOAA (McCord et al. 2018), NAFION BP2 (Gui et al. 2023), OBS (Bao et al. 2017).

Compound	Structural formula
HFPO-DA	
HFPO-TA	
HFPO-TeA	
PFMOAA	

Nafion BP2	
OBS	

3.1.2.2 Polyfluoroalkyl substances

Polyfluoroalkyl substances are substances widely used in industry (Liu & Mejia-Avendaño 2013). Like perfluoroalkyl substances, they contain a functional group attached to a carbon chain in their molecule (OECD Undated). Hydrogen atoms are partially replaced by fluorine atoms in the carbon skeleton (Ramírez Carneo et al. 2021). The resulting molecule contains a fully fluorinated chain that is broken at some point by a carbon atom containing hydrogen atoms, not fluorine. At the carbon-hydrogen bond site, the polyfluoroalkyl substance molecule can be transformed by microorganisms or abiotic influences. Thus, fully fluorinated parts of the chains may be released into the environment. Because of this, polyfluoroalkyl substances are referred to as PFAA precursors (Buck et al. 2011; Liu & Mejia Avendaño 2013).

The subclass Polyfluoroalkyl substances is divided into 6 groups (see Figure 1):

- fluorotelomer substances,
- perfluoroalkane sulfonamide substances (name perfluoroalkane refers to fully fluorinated carbon chain tail, there are 2 more CH₂ groups without fluorine),
- polyfluoroalkyl ether acids (PolyFEA),
- chloropolyfluoroalkyl ether acids,
- chloropolyfluoroalkyl acids,
- polyfluoroalkyl carboxylic acids (PolyFCA).

Some groups are further subdivided into subgroups (alcohols, carboxylic acids, sulfonic acids) according to the functional group in the molecule (Liu & Mejia Avendaño 2013; CLU-IN 2023). Polyfluoroalkyl substances are also used as substitutes for banned PFAS (ITRC 2023).

3.2 Structure of commonly known PFAS

The two different parts of PFAS molecules (carbon-fluorine tail, functional group) will be described in the following subsections.

3.2.1 Carbon – fluorine tail

The bond between the carbon atom and the fluorine atom gives the whole PFAS molecule high chemical, biochemical and thermal stability (Ghisi et al. 2019; Wang et al. 2020a). This

stability is due to the atomic structure of the fluorine atom, mainly because of the larger size of the fluorine atom compared to the hydrogen atom and the strong bonding between these atoms (Ghisi et al. 2019; Leung et al. 2023). This strong bonding between fluorine and carbon atoms is called a covalent bond and reaches values of 110 kcal/mole (Wang et al. 2020a). Ghisi et al. (2019) report covalent bond strengths ranging from 109 to 130 kcal/mol. The covalent bond between carbon and fluorine (the most electronegative element) is considered the strongest bond in organic chemistry (Kissa 2001; Leung et al. 2023). Due to the strength of the bond, which increases as the number of fluorine atoms bonded to the central carbon atom increases, this part of the molecule is considered non-reactive (Ghisi et al. 2019; Leung et al. 2023).

The presence of fluorine atoms in the PFAS carbon chain also causes very weak intramolecular and intermolecular interactions. This makes PFAS more volatile and has a lower boiling point compared to hydrocarbons of similar molecular weight. These weak intermolecular interactions are also responsible for the low surface tension of PFAS, making PFAS have excellent surface wettability (Leung et al. 2023).

The persistence in the environment is strongly influenced by the length of the hydrophobic carbon chain. PFAS with a longer chain (i.e., more than 5 carbon atoms in the chain) can have higher octanol-water (K_{ow}) coefficient values than PFAS with a shorter chain. An increasing K_{ow} value reflects increasing persistence in the environment (Ghisi et al. 2019). Mei et al. (2021) analyzed the persistence of PFAS in the environment using the sorption coefficient K_d . The K_d value increased with increasing carbon-fluorine chain length. The increased adsorption of PFAS with a longer CF chain to the soil surface was also confirmed by CLU-IN (2023). Varying the carbon chain length also affects the (partitioning) behavior of molecules that lie between the hydrophobic and hydrophilic phases. For this reason, shorter molecules are generally more soluble in water than molecules with a higher number of carbon atoms in the chain (CLU-IN 2023).

Based on the number of carbon atoms in the molecule, PFAS can be divided into short-chain PFAS and long-chain PFAS (Kuzniewski 2022). The boundary between the short and long chain is 6 carbon atoms in the molecule (Krahn et al. 2023). Ghisi et al. (2019) referred to PFCA with a chain shorter than 7 carbon atoms as short-chain compounds. PFSA are classified as short if they have less than 6 carbon atoms in the molecule. The most discussed and mentioned PFOS and POFA (which are the best-known representatives of the PFAS group) are classified as long-chain PFAS. Both of these representatives contain 8 carbon atoms in the main chain (Buck et al. 2011). Some PFAS with lower carbon numbers are less likely to accumulate in living organisms. However, like long-chain PFAS, these short-chain PFAS are also difficult to degrade. Short PFAS are less easily sorbed to the solid soil phase. This leads to their high mobility in the environment (Ghisi et al. 2019). Short-chain PFAS compounds can not only be industrially produced but can also be formed by dissolving more complex PFAS in the environment (American Water Works Association 2019).

3.2.2 Functional group

The functional group is localized at the end of the PFAS molecule and is responsible, unlike the non-reactive C-F chain, for the reactivity of the entire molecule. The reactivity can also be influenced by the non-fluorinated part of the molecule, which is not part of the functional

group (Ghisi et al. 2019). The hydrophilic functional group together with the hydrophobic and lipophobic CF tail form two specific structures typical of PFAS (Wang et al. 2020a; Mei et al. 2021). These two different natures of one molecule cause the molecule to behave differently in different media and split the molecule between two phase interfaces (CLU-IN 2023).

Most of the functional groups in PFAS molecules are anionic at pH 4-9, which is normal for the environment (Mei et al. 2023). They are therefore negatively charged and will be repelled from negatively charged surfaces and attracted to positively charged ones. Some functional groups of PFAS have a positive charge, thus we refer to them as cations. There are also PFAS compounds that contain both anionic and cationic functional groups in one molecule. These compounds, called zwitterions, will exhibit partitioning behavior between environments with different charges (CLU-IN 2023).

Due to the high variability in the length of the hydrophobic and lipophobic (hydrophilic and lipophilic) alkyl chain (CF chain) and the charge of the hydrophilic functional groups that can be attached to the molecule, it is difficult to estimate the behavior of PFAS in the environment compared to older persistent organic pollutants (CLU-IN 2023; Krahn et al. 2023).

3.3 Use of PFAS in industry

These substances began to be used in industry in the 1950s as a result of the boom in fluorine chemistry (Buck et al. 2011; Munoz et al. 2019). Some sources date the beginning of use to the 1940s (Wang et al. 2020a).

This broad group of substances with unique properties was and still is widely used in many industries (Huang et al. 2019; Wang et al. 2020a; Agency for Toxic Substances and Disease Registry 2022). PFAS has found application in the production of surfactants (they reduce the surface tension of the water), adhesives, coatings, paints, lubricants, pesticides, food packaging, or aqueous firefighting foams (Wang et al. 2020a; Xu et al. 2021; Leung et al. 2023). PFAS are also added as additives to polymers (Xu et al. 2021), used in the surface treatment of textiles and paper, in photolithography, and chromium plating (Huang et al. 2019; Mei et al. 2021).

Substitutes for banned PFAS have been increasingly used in industry in recent years. OBS is widely used in China (Xu et al. 2021) as a cheap substitute for PFOS in plating, in the production of fire-fighting foam (Bao et al. 2017; Lohmann & Letcher 2023), or in the manufacture of fluoroprotein foams and alcohol-resistant foams (Huang et al. 2021). In China, the compound F-53B is also used as a substitute for PFOS (Munoz et al. 2019). This substance, utilized in the electroplating industry, has gained importance since the 1970s due to its low price (Hu et al. 2021; He et al. 2022). GenX, produced in the USA, is used in the same industries and the production of the same or similar fluoropolymer products as the PFOA, which it replaced (EPA 2023c). Kancharla et al. (2022) mention the specific use of GenX in the production of surfactants. At the same time, GenX can be released as a by-product during the manufacture of fluoromonomers (Hopkins et al. 2018). Nafion BP2 is released during the production of the Nafion membrane, which is used in the production of electrochemical cells (Gui et al. 2023).

3.4 PFAS entrances into the environment

Due to widespread use, these persistent substances have entered all components of the environment, including biota, where they accumulate and have a toxic effect on living organisms (Buk et al. 2011; Ghisi et al. 2019; Wang et al. 2020; Sørmo et al. 2021). PFAS entered the environment during production or use or spread from local point sources. Local resources include:

- fluorochemical plants,
- firefighting training facilities,
- metal and paper industry,
- landfills,
- wastewater treatment plants.

PFAS can also escape from fields where biosolids containing PFAS have been applied (Ghisi et al. 2019; Sørmo et al. 2021). However, this source is referred to as diffuse and not a point source (Sørmo et al. 2021). The use of aqueous film-forming formulations during firefighting was also an extensive source of soil contamination near civilian and military airports (Liu & Mejia Avendaño 2013; Kancharla et al. 2022).

PFAS has been spread by both point and diffuse sources through surface and groundwater as well as air far from pollution sources (Liu & Mejia Avendaño 2013; Sørmo et al. 2021; Xu et al. 2021). They have been detected in soils worldwide, including rural areas. PFAS have also been detected in the Arctic, where they were transported by atmospheric transport (Ghisi et al. 2019; Wang et al. 2020; Sørmo et al. 2021). PFAS enter agricultural soil together with irrigation water or after the application of sewage sludge. Through the consumption of plants grown in contaminated soil, PFAS reaches animals and humans (Ghisi et al. 2019; Mei et al. 2021).

Due to the global spread of these bioaccumulative, biotoxic, and resistant to degradation substances, perfluorocarboxylic and perfluorosulfonic acids have been gradually restricted (Munoaz et al. 2019; Gui et al. 2023). Most substitutes for banned PFAS are still organofluorine chemicals (Bao et al. 2017). Nevertheless, reduced bioaccumulation of PFAS substitutes containing one or more alkyl ether bonds in a fully fluorinated carbon chain can be assumed (Munoz et al. 2019). According to the Madrid Statement, these substitutes also raise concern due to their potential persistence in combination with the lack of information on their toxicity (Bao et al. 2017; Conley et al. 2019; Munoz et al. 2019). Leung et al. (2023) identified the unrestricted production of short-chain PFAS and their subsequent accumulation in the environment as a growing global problem.

The toxicity of the F-53B substitute has been monitored since 2013 when this component was first detected in the environment (surface and groundwater, seawater, atmosphere, sediments, sewage sludge) (Munoz et al. 2019; He et al. 2022; Xu et al. 2022). However, this substitute has been leaking into the environment since the 1970s. Specifically, the F-53B was found in China, where this substance is used, but also in the USA, the Netherlands, Germany, Great Britain, and South Korea. In some Chinese rivers, the concentration of F-53B was higher than PFOS (He et al. 2022). At the same time, the persistence of the substitute was proven, and its toxicity was identified. Based on research, the acute toxicity of F-53B is considered to be comparable to the acute toxicity of the banned PFOS.

GenX and ADONA substitutes, which have been detected in water in Asia and Europe, are also subject to increased monitoring (Munoz et al. 2019; EPA 2023b). GenX was first detected in the rivers Elbe and Rhine in Germany, in the delta of the rivers Rhine and Meuse in the Netherlands, and in the Xiaoqing River in China (Xu et al. 2021). High concentrations of GenX have been observed in the Cape Fear River, drinking water in North Carolina, and Spring Lake. However, GenX is likely being released into water in other parts of the USA. The West Virginia Department of Environmental Protection has allowed the release of GenX into the Ohio River if the concentration does not exceed 17,500 ng/L. However, this concentration has already been exceeded several times (Hopkins et al 2018). GenX was also found in sewage sludge in the Czech Republic. In roughly 20% of the samples, shorter PFAS (including GenX) was found compared to the otherwise abundant PFOS and PFOA, which indicates the restriction of long PFAS (Semerád et al. 2020). However, GenX has been found to be more toxic than PFOA (Xu et al. 2021).

A high bioaccumulation capacity was also observed for the substitute Nafion BP2. This substitute was first detected in 2017 in surface water in the USA (Gui et al. 2023), specifically in North Carolina (Conley et al. 2022). OBS has also already been detected in water, specifically in water samples taken from an urban wastewater treatment plant in northern China and around the Daqing oil field (Bao et al. 2017; Huang et al. 2021). The distribution of OBS in the tissues of wild crucian carp was comparable to the distribution of PFOS, but the substitute accumulated less in the tissues (Huang et al. 2021)

HFPO-TeA is not only a separately used substitute for PFOA but also a by-product produced during the production of GenX. Increased production of this substitute also leads to increased emissions of HFPO-TeA. This substance has been detected in soil and surface water (Dong et al. 2023). HFPO-TA is released into the environment from the process of producing fluorinated polymers. This substitute has also been detected in soil, sediments, surface, and groundwater and, unlike HFPO-TeA, also in living organisms (Dong et al. 2023; Sun et al. 2023).

3.5 PFAS in soils

Soil is an important reservoir of PFAS in the environment (Mei et al. 2021). Contaminated plants grown on it are the main source of PFAS contamination for humans (Kancharla et al. 2022). Due to high concentrations of PFAS in soil (PFAS concentrations were often measured in values several mg.kg⁻¹ soil), it is necessary to know the sorption mechanisms and mobility of PFAS in soil (Fabregat-Palau et al. 2021). In soil, PFAS can be absorbed into soil particles or dissolved in the soil solution. The sorption capabilities of PFAS are important in determining the concentration of PFAS available to plants. Only PFAS contained in the solution can be taken up by plants, specifically their roots (Mei et al. 2021). The roots are, according to Wang et al. (2020a) and Wang et al. (2020b), the primary pathway through which PFAS enter plants. Sorption, which is conditioned by PFAS structure and soil properties (Mei et al. 2021), will be described in the next chapter.

3.5.1 PFAS sorption in soil

The sorption of PFAS in soil is influenced by several factors. According to Pereira et al. (2018) and Ghisi et al. (2019), the most significant factor affecting PFAS sorption in soil is the content and quality of organic matter. Li et al. (2019), Mei et al. (2021), and Sørmo et al. (2021) consider the most important PFAS sorbent to be total organic carbon (TOC), which is, however, often considered a correlated quantity to soil organic matter (SOM) (Mei et al. 2021). TOC proved to be a possible sorbent for two of the most well-known representatives of PFAS, i.e. PFOA and PFOS. For other representatives of PFAS (i.e. perfluoropentanoic acid or PFPeA, perfluorodecanoic acid or PFDA, and PFBS) it has not been proven that TOC is the dominant parameter affecting their sorption in soil (Li et al. 2019).

Sorption of PFAS in the soil is not only determined by organic matter (Pereira et al. 2018), but other factors also influence sorption, such as:

- pH,
- temperature,
- salinity of divalent ions,
- presence of soil bacteria that can sorb (not metabolize) PFAS with electrostatic or hydrophobic forces (Wang et al. 2020b; Fabregat-Palau et al. 2021; Mei et al. 2021).

Soil structure, specifically the presence of micropores, also plays a role in PFAS sorption. PFAS are strongly sorbed in micropores ranging in size from a few angstroms (Å) to several hundred angstroms. From meso- and macropores, PFAS are more easily released into the soil solution (Mei et al. 2021).

The bonds that can form between PFAS and the soil solid phase, which will be further described, are shown in Figure 2.

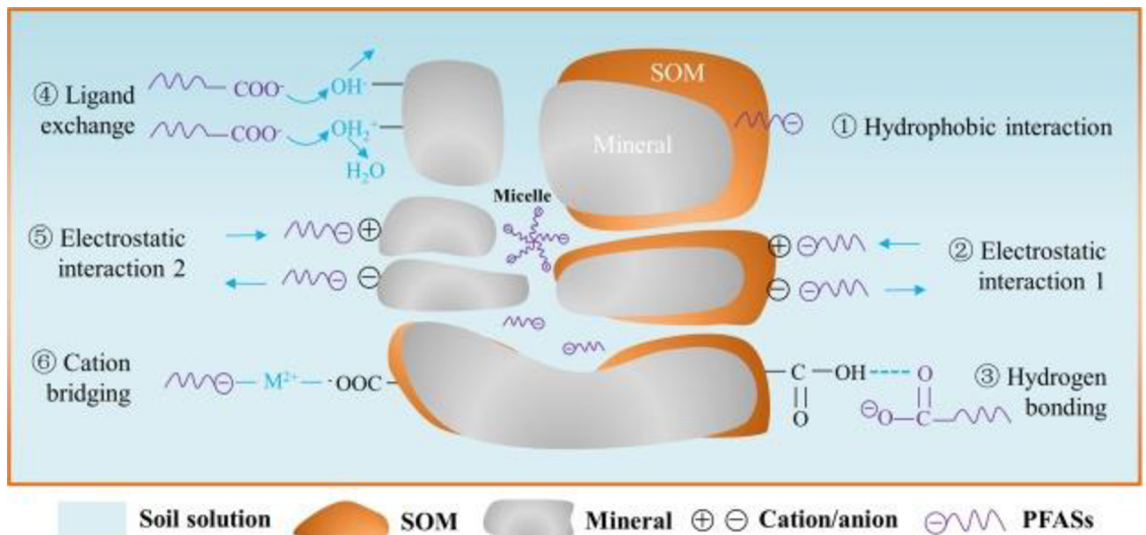


Figure 2. The bonds between PFAS and inorganic and organic soil fraction (Mei et al. 2021).

3.5.1.1 Sorption on the organic part of the soil

Organic matter primarily consists of organic humic substances (humic acid, fulvic acid, humine) (Fabregat-Palau et al. 2021), which play various roles in the sorption of PFAS in soil (Mei et al. 2021).

The first type of interaction between PFAS and SOM is the bond between the hydrophobic CF chains in the PFAS molecule and the aliphatic and aromatic groups contained in the soil organic matter. These aliphatic and aromatic groups are also hydrophobic (Mei et al. 2021). Humic acid contributes the most to hydrophobic reactions between soil organic matter and PFAS, unlike fulvic acids and humic acids (Pereira et al. 2018). However, hydrophobic interactions can also occur between humic acid and PFAS contained in the soil. In this case, hydrophobic carbon-fluorine chains are bound to hydrophobic cavities on humic acids (Li et al. 2019). According to Fabregat-Palau et al. (2021), hydrophobic interactions are an important mechanism of PFAS sorption onto humic acids.

The second type of interaction between PFAS and organic matter involves electrostatic interactions. At normal pH, the anionic functional groups of PFAS are attracted to positively charged amino and amide groups contained in organic matter (Mei et al. 2021). At the same time, these functional groups are repelled from positively charged phenolic and carboxylated functional groups in organic matter (Pereira et al. 2018; Mei et al. 2021).

The penultimate bond formed between soil organic matter and PFAS is hydrogen bonding (Mei et al. 2021). This bond involves oxygen contained in carboxylic or functional groups and hydroxyl groups contained in soil organic matter (Fabregat-Palau et al. 2021; Mei et al. 2021).

The last bond between PFAS and organic soil matter involves cationic bridges. These bridges are formed in soils that contain many carboxyl groups. These soil carboxyl groups can bind metal ions, with which the carboxyl or sulfone functional group of PFAS subsequently interacts. This interaction can be written as follows: SOM-metal-PFAS. Ca^{2+} and Mg^{2+} ions can form cationic bridges with the carboxyl functional groups of PFCA. With the sulfone groups of PFSA, cationic bridges form Ca^{2+} ions (Mei et al. 2021).

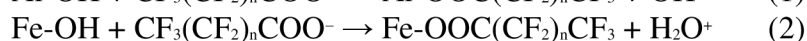
3.5.1.2 Sorption on mineral part of soil

Sorption of PFAS to the inorganic soil fraction plays a significant role in the sorption of PFAS in soil, as minerals constitute a considerable portion of soil compounds (Mei et al. 2021). The positive effect of PFAS sorption on the mineral fraction of the soil has also been described by Fabregat-Palau et al. (2021) in soils with organic carbon content below 5%. The interaction between PFAS and the soil mineral fraction is mediated by titanium, iron, and aluminum oxides (Fabregat-Palau et al. 2021), with iron oxides playing a dominant role (Li et al. 2019). Sorption of PFAS onto aluminum oxides varied depending on the PFAS sorbed. PFPeA, PFDA, and PFBS were better sorbed on aluminum oxides compared to PFOA and POFS (Li et al. 2019).

The first type of bond between PFAS and mineral particles is similar to organic matter, electrostatic interactions. This bond is influenced by pH and mineral type. If the soil pH is lower than 6, the Al_2O_3 in the soil becomes positively charged and attracts the anionic functional group of PFAS (Mei et al. 2021). The surfaces of iron oxides are also positively charged (Li et al. 2029). Sandy soils predominantly containing SiO_2 , which are negatively charged at pH 6,

repel anionic functional groups of PFAS. SiO₂ would only become positively charged when the pH drops below 2. Electrostatic interaction between Al₂O₃ and PFAS, as well as PFAS interaction with other soil minerals, may not be stable. Nevertheless, there is a significant interaction between PFAS with a sulfone functional group and the mineral fraction of soil (Mei et al. 2021).

The second type of interaction involves the exchange of ligands between hydroxyl groups in soil minerals such as goethite (α -FeOOH) or gibbsite (Al(OH)₃) and the carboxyl group of PFAS. The process of ligand exchange between PFAS and goethite and gibbsite are described in equations 1 and 2.



Li et al. (2019) and Mei et al. (2021) identified ligand exchange at iron oxides as one of the main mechanisms of PFAS sorption in soil.

Li et al. (2019) mention another type of interaction, the formation of hydrogen bridges (hydrogen bonding) between PFAS and the mineral fraction of the soil. Hydrogen bridges are formed between the oxygen contained in the functional group of PFAS and the hydroxyl group contained in aluminum and iron oxides.

3.5.2 Properties of PFAS affecting soil sorption

Due to their specific properties, PFAS behave differently in soil compared to other organic substances (Li et al. 2019). Organic substances, or contaminants, are hydrophobic substances without a charge. PFAS, on the other hand, contain a charge and are also hydrophobic and hydrophilic at the same time (Li et al. 2019; Mei et al. 2021). These properties must be reflected when describing the behavior of PFAS in soil and their subsequent transport to plants (Mei et al. 2021).

PFAS are generally referred to as substances with a low sorption potential (Wang et al. 2020a). Their ability to sorb onto soil particles or release into the soil solution is influenced by the length of the carbon chain in the PFAS molecule (Mei et al. 2021). Short PFASs and PFCAs are more poorly sorbed in soil. These substances are more soluble and therefore more mobile in the environment (Ghisi et al. 2019; Wang et al. 2020a). Specific examples of different sorption of PFAS representatives are given in their work by Fabreagat-Palau et al. (2021). Low sorption capacity to soil particles was observed for PFBA, PFBS, and PFHxA, while PFHxS, PFOA, PFOS, and PFNA were better sorbed. Longer-chain PFAAs are more likely to form (hemi)micelles. These micelles increase the size of the compound, resulting in a decrease in hydrophobicity. Compounds with lower hydrophobicity are less sorbed to soil particles and are better accepted by plants (Mei et al. 2021).

Sorption of PFAS in soil is influenced by the functional group present (Wang et al. 2020a) and the charge that this group carries (Mei et al. 2021), in addition to the length of the CF chain. More PFAS with a sulfone functional group is sorbed on soil particles compared to PFAS with a carboxyl functional group, even with the same number of carbon atoms in the chain (Ghisi et al. 2019; Li et al. 2019; Wang et al. 2020a). The difference in PFAS sorption in the soil can be partially explained by the different bioaccumulation potentials of PFAS in plants, as plants take

up homologs with a carboxyl functional group more (Wang et al. 2020a). In terms of charge, negatively charged PFAS represent the greatest danger to the environment, as they have the lowest value of the sorption coefficient K_d . Positively charged PFAS, zwitterionic PFAS, and uncharged PFAS are better sorbed onto soil particles (Mei et al. 2021).

3.6 PFAS in plants

Uptake of PFAS by plants, specifically through their roots, has been observed in many plant species. Apart from the roots, plants are also able to take up PFAS through the above-ground biomass, albeit to a minimal extent (Wang et al. 2020a). In the atmosphere, PFAS with short chains are found in higher concentrations. These short PFAS can be found in two forms. In the first case, PFAS can be bound to solid particles. In the second case, they can be in the vapor phase, even if they have a low vapor pressure (Jin et al. 2018).

3.6.1 PFAS in root

Roots play a major role in the uptake of nutrients needed by plants. Along with nutrients, the roots can also absorb contaminants, including PFAS, which are found in the soil (Wang et al. 2020a; Colomer-Vidal et al. 2022). The exact mechanism of PFAS transport into plants is not yet fully understood and requires further research in this area (Wang et al. 2020a; Wang et al. 2020b). Only certain aspects of this transport are known. PFAS dissolved in the soil solution (Mei et al. 2021) move to the root based on the concentration gradient (Wang et al. 2020a; Mei et al. 2021) and the water potential gradient, which arises resulting in plant transpiration (Mei et al. 2021; Colomer-Vidal et al. 2022). Transpiration generally plays an important role in the uptake of xenobiotic substances by plants (Wang et al. 2020a).

The actual passage of PFAS into plants, according to Wang et al. (2020b), Zhang et al. (2020), and Xu et al. (2022), occurs through diffusion via carriers (water channels, sometimes called aquaporin channels and anion channels) (Wang et al., 2020b; Mei et al., 2021; Xu et al., 2022). This energy-independent process runs in the direction of the energy gradient (Wang et al. 2020b). However, according to Wang et al. (2020b), terrestrial plants are also able to absorb PFAS actively, i.e. with the use of energy. This process is again mediated by membrane carriers, whose size is greater than the average bond length between fluorine and carbon atoms, which is approximately 1.35 Å. The diameter of the narrowest water channel is 2.8 Å, and the average size of the anion channel is even larger. Wang et al. (2020a) and Mei et al. (2021) confirmed the ability of plants to actively absorb PFAS, depending on the plant species and the type of PFAS. In the case of corn, active transport of PFOA was observed, but not PFOS; while in wheat, both compounds were actively transported to the root of the plant.

Once PFAS are absorbed by the root epidermis (Zhang et al. 2020; Xu et al. 2022), these compounds are transported through various routes through the cortex, and endodermis into the vascular root tissues of the plant (Wang et al. 2020a; Mei et al. 2021; Xu et al. 2022). Wang et al. (2020a), Zhang et al. (2020), and Xu et al. (2022) mention 2 transport pathways of PFAS into the plant's vascular tissue:

- apoplastic pathway,
- symplastic pathway.

Mei et al. (2021) also mention the transmembrane pathway in their work. If PFAS move outside the cells along the cell walls, this is the apoplastic pathway. The symplastic pathway describes the movement of PFAS through plasmodesmata in the cell (Mei et al. 2021; Xu et al. 2022). The transmembrane pathway refers to the transport of PFAS through cell membranes and cells (Wang et al. 2020b; Mei et al. 2021). The transport of PFAS into the plant's vascular root tissue is shown in Figure 3.

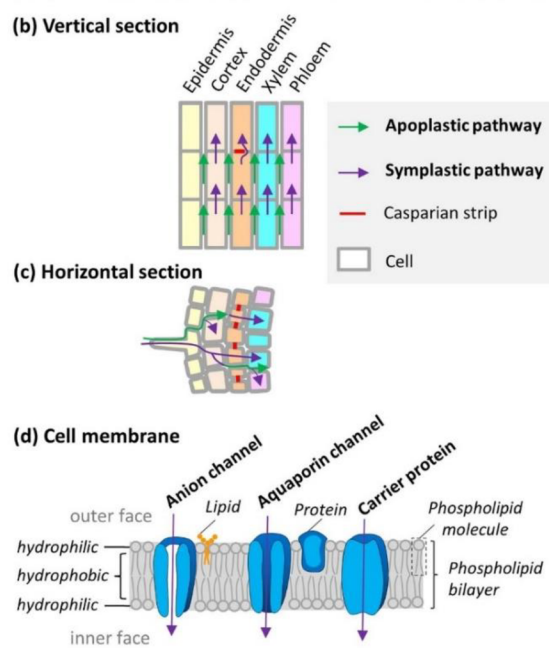


Figure 3: Possible transport of PFAS into the plant root (modified from Mei et al. 2021).

After reaching the vascular root tissues, i.e. phloem and xylem (Mei et al. 2021), PFAS are transported via transpiration stream in the xylem to the aboveground parts of the plant (Wang et al. 2020a; Zhang et al. 2020). However, Mei et al. (2021) and Xu et al. (2022) pointed out that PFAS can also be transported through the phloem. From the mechanism of transpiration, it can be inferred that PFAS will accumulate in vegetative organs that absorb more water, and at the same time contain enough sorption sites for the binding of contaminant molecules (Wang et al. 2020a).

3.6.2 PFAS in aboveground biomass of plant

PFAS transported by xylem tend to accumulate in the shoot (Zhang et al. 2020), specifically in the leaf (Wang et al. 2020b; Mei et al. 2021). As a result of transpiration, PFAS molecules remain in the leaves, while water molecule transition into the atmosphere (Wang et al. 2020b; Mei et al. 2021). Phloem-transported PFAS reach the fruit (Mei et al. 2021).

Dissolved PFAS can be gradually absorbed by cell walls in roots, stems, and leaves. Part of PFOS and PFOA can pass through the cell walls and get through the cell membrane to the organelles. Organelles containing 15-30% lipids and cell walls play an important role in the storing of poorly soluble lipophilic organic pollutants. Nevertheless, PFAS were more represented in the soluble phase. The reason could be the repulsion of anionic PFAS from the negatively charged cell walls. PFOS accumulated better in cell walls and organelles of leaves

and roots compared to PFOA. PFOA was much more represented in the soluble fraction. This distribution of PFOA did not match the behavior of poorly soluble lipophilic contaminants (Wang et al. 2020b).

3.6.3 What affects the uptake and movement of PFAS in plants?

The transport of PFAS from the soil to the root and then through the vascular root tissue to the aboveground biomass is influenced by several factors. This movement is influenced by:

- the environment (or abiotic factors),
- plant physiology,
- the PFAS molecule Ghisi et al. 2019; Wang et al. 2020a; Zhang et al. 2020; Mei et al. 2021).

Wang et al. (2020a) and Wang et al. (2020b) include as factors also the duration of PFAS exposure to plants.

3.6.3.1 Abiotic factors

Environmental influences can include variables such as pH, salinity, and soil temperature (Ghisi et al. 202019; Wang et al. 2020a; Wang et al. 2020b; Zhang et al. 2020). The influence of organic matter and generally soil properties, which the mentioned authors also consider important for understanding the movement of PFAS in the environment, has been described in previous chapters.

An increase in temperature can accelerate transpiration and metabolism, resulting in higher uptake and accumulation of contaminants in plants (Ghisi et al. 2019; Wang et al. 2020a; Mei et al. 2021). With a temperature increase of 10 °C from 20 to 30 °C, PFAS accumulation in the plant increased 1.5-2.3 times. The uptake of longer PFAS was more affected by the change in temperature (Wang et al. 2020a). Mei et al (2021) observed an increase in the concentration of all tested PFCA with increased temperatures, but longer-chain PFCA accumulated more rapidly.

An increase in salinity has the opposite effect on transpiration compared to an increase in temperature. With a decrease in transpiration, the plant receives less water, and thus fewer nutrients and contaminants in water. However, the opposite trend was observed in hydroponic experiments. With increases in salinity, plants took up more PFAS. The reason could be physiological changes in plants or changes in the physico-chemical properties of PFAS.

The effect of pH on PFAS uptake has not yet been fully explained, but a higher uptake of short-chain PFAS (e.g. PFBA, PFHxA) was observed with increasing pH (Wang et al. 2020a). Mei et al. (2021) relate pH to plant growth. A pH value around 6 is optimal for plant growth, resulting in rapid uptake of PFAS.

The initial concentration of PFAS in the soil (Ghisi et al. 2019; Wang et al. 2020a; Wang et al., 2020b) as well as their accessibility (Zhang et al. 2020) also play a significant role in plant uptake of PFAS. Zhang et al. (2020) observed an increase in PFAS in plant parts together with an increase in soil PFAS concentration.

The behavior of PFAS in the environment is also influenced by the length of time they spend in the soil. Reduced availability of PFAS to plant roots over time has been observed as these contaminants are sequestered in the soil (Wang et al., 2020a; Wang et al., 2020b).

3.6.3.2 Plant

The plant species and its physiology (specifically the presence of the Casparian strip and the content of proteins and lipids in the root) also influence PFAS transport into the plant (Ghisi et al., 2019; Wang et al., 2020b; Mei et al., 2021; Xu et al., 2022), as well as the growth phase (Wang et al., 2020a). Differences between plants lead to different rates of transpiration, resulting in significant variations in PFAS accumulation across plant species (Wang et al. 2020a).

The influence of plant species on PFAS transport and accumulation was studied by Mei et al. (2021). In zucchini, PFPeA was transported by xylem and subsequently accumulated in leaves. In hydroponically grown tomatoes, PFPeA was transported by the phloem and accumulated in the fruit.

The influence of the Casparian strip on PFAS transport in the root was investigated by Wang et al. (2020a), Wang et al. (2020b), and Mei et al. (2021). Casparian strips are structures made of hydrophobic suberin and lignin that prevent the transport of water with dissolved PFAS between cells from the cortex to the vascular root tissues of the plant (Wang et al. 2020b). PFAS with longer chains penetrate these Casparian strips less effectively. Therefore, longer PFAS molecules tend to accumulate in the root, while shorter-chain PFAS may accumulate more in the aboveground parts of the plant (Wang et al. 2020a). For plants that do not have a Caspian strip in the root (radish, carrot), higher contaminant transport into the aboveground biomass is expected, regardless of the length of the CF chain (Mei et al. 2021).

The lipid and protein content in the plant root also plays a significant role in PFAS uptake. These substances, whose content varies depending on the plant species, can interact with PFAS in ionic form through electrostatic and hydrophobic interactions. These interactions play a key role in PFAS uptake into the plant root (Xu et al. 2022). Wang et al. (2020a) and Colomer-Vidal et al. (2022) observed an increase in the concentration of longer PFAS molecules (PFOA, PFOS) with increasing protein content. The opposite trend was observed with increasing lipid content in the root (Wang et al. 2020a).

3.6.3.3 PFAS molecule

The properties derived from the structure of this molecule also play an important role in the transport of PFAS. The movement of the plant is influenced by:

- length of CF chain,
- present functional groups,
- water solubility
- volatility (Wang et al. 2020a; Mei et al. 2021).

The number of carbon atoms in the chain together with the molecule's structure (linearity vs. branching) influences the mobility of PFAS not only in the soil but also in the plant (Ghisi et al. 2019; Wang et al. 2020a; Colomer-Vidal et al. 2022; Xu et al. 2022). PFAS with longer chains are less bioavailable to plants as they are more sorbed to soil particles. In contrast, PFAS with shorter chains, due to their smaller molecular size and higher solubility, can penetrate plant layers (e.g. the epidermis, cortex, endodermis, and pericycle) into the vascular bundle. The boundary between shorter and longer molecules varies among authors. According to Ghisi et

al. (2019) and Colomer-Vidal et al. (2022), PFAS with 4 to 6 carbons (PFBA, PFPeA, and PFHxA) are accumulated in leaves and fruits, longer molecules in the root (PFOA, PFOS). According to Zhang et al. (2020), PFCA with more than 6 carbon atoms and PFSA with more than 4 carbon atoms in the chain accumulate in the root. Xu et al. (2022) observed root accumulation of PFCA with 7 or more carbons in the chain and PFSA with more than 6 carbons in the main chain.

The solubility of the molecule is also influenced by its structure. It has been found that branched forms of PFOS and POFA are more transported than linear isomers, due to their lower hydrophobicity compared to linear PFAS (Mei et al., 2021; Xu et al., 2022). Therefore, it is possible to assume that short and branched PFAS molecules will be preferentially transported and accumulated (Xu et al., 2022).

The sorption capacity of PFAS in plants is influenced by more than chain length, it is also affected by the main functional group (Ghisi et al. 2019; Wang et al. 2020a). PFAS with a carboxyl functional group is significantly more accumulated in plants than the same-length PFAS with a sulfone functional group (up to 100 times higher accumulation in potatoes, oats, or maize). In contrast, PFAS with a sulfone functional group is about 1.7 times more accumulated in soil (Wang et al. 2020a). This reduced accumulation of PFSA in plants is probably due to the larger size and hydrophobicity of PFSA molecules. The uptake of PFAS by plants can also be influenced by other functional groups (-NH-, -OH) in the molecule (Mei et al. 2021).

3.7 Biochar as PFAS remediation agent

Efforts to prevent the release of PFAS from the soil and the subsequent contamination of surface and groundwater have been the subject of research for several decades. The optimal solution appears to be the use of carbon-based sorbents. They can effectively immobilize organic contaminants on their surfaces, resulting in their reduced release into the environment (Sørmo et al. 2021). Today, activated carbon and biochar are used as PFAS sorbents (Sørmo et al. 2021). Activated carbon, produced from anthracite, is currently the most commonly used PFAS sorbent in the soil. However, its production is energetically and chemically expensive. That is the reason, why biochar has been recently used. The advantage of this sorbet is greater sustainability compared to activated carbon (Sørmo et al. 2021; Krahn et al. 2023).

In addition to the sorption of inorganic and organic contaminants in the soil (Yaashikaa et al. 2020), biochar can be used for carbon sequestration, wastewater treatment, energy production, catalysis, or soil quality improvement (Yaashikaa et al. 2020; Thoma et al. 2022).

3.7.1 Production of biochar

Biochar is a solid carbonaceous residue (Sørmo et al. 2021) formed during several types of processes:

- hydrothermal carbonization
- gasification
- flash carbonization
- torrefaction
- pyrolysis (the most commonly used process) (Yaashikaa et al. 2020).

All these processes are thermochemical decomposition occurring at elevated temperatures and without access to oxygen (Hu & Gholizadeh 2019). Many raw materials can be pyrolyzed (Thoma et al. 2022). Agricultural residues (rice straw, wheat straw, waste wood, sugar beet tailings, corn cob) (Yaashikaa et al. 2020), sewage sludge (Thoma et al. 2022; Krahn et al. 2023), food waste, waste tires, and waste mixtures are most often pyrolyzed (Sørmo et al. 2021).

During pyrolysis, three products are generated:

- biochar,
- hydrogen-rich synthesis gas (syngas),
- pyrolysis oil (sometimes named even as bio-oil) (Hu & Gholizadeh 2019; Thoma et al. 2022).

Pyrolysis takes place under various conditions, resulting in biochars with different physicochemical properties (Sørmo et al. 2021). Conditions that affect the biochar properties are:

- temperature of pyrolysis,
- heating speed,
- pyrolysis duration.

The properties of biochar are also influenced by the processed material. When comparing pyrolysis with classical combustion, it is evident that apart from the different conditions, different end products are also created. Pyrolysis produces biochar with many interesting properties, while combustion generates ash. At the same time, less carbon, nitrogen, and sulfur oxides are released during pyrolysis compared to the combustion of waste materials (Thoma et al. 2022).

The average temperature of the pyrolysis process ranges from 300 °C to 700 °C (Hu & Gholizadeh 2019). Thomas et al. (2022) reported an average pyrolysis temperature range from 500 °C to 800 °C. The widest range of temperatures is reported by Yaashikaa et al. (2020), namely 250 to 900 °C. The temperature increase during the process is rapid. Pyrolysis process takes place under atmospheric pressure (Hu & Gholizadeh 2019).

The temperature of the process affects the resulting specific surface area of biochar. To achieve a significant porosity and a sufficiently large specific surface area of the biochar, a temperature of at least 600 °C is required. With increasing pyrolysis temperature, the ability of biochar to sorb PFAS on its surface increases, but the yield of biochar decreases (Sørmo et al., 2021). The adsorption of PFAS on biochar is also influenced by functional groups on the biochar surface or the cation exchange capacity (Yaashikaa et al. 2020). The physicochemical properties of biochar can be modified by the addition of acidic, alkaline, or oxidizing agents which alter the biochar surface (Yaashikaa et al. 2020).

3.7.2 Pyrolysis process

During pyrolysis, water evaporation occurs first at a temperature of around 100 °C, which results in a reduction in the weight of the input material (Yaashikaa et al. 2020). This is followed by the degradation of large molecules into smaller ones. The decomposition of cellulose occurs

at temperatures between 305-375 °C. Cellulose is first depolymerized to form levoglucosan, which is further converted into hydroxymethyl furfural through dehydrogenation. This substance can further decompose into liquid and gaseous products such as carbon monoxide, carbon dioxide, hydroxyacetaldehyde, hydroxyacetone, and acetaldehyde. Hydroxymethyl furfural can also undergo several reactions (aromatization, condensation, and polymerization) to re-form solid biochar. The decomposition of hemicellulose follows a similar process to cellulose but at temperatures of 200-350 °C. Hemicellulose is initially depolymerized into oligosaccharides. These are subsequently transformed into biochar through a series of transformations or broken down into syngas and pyrolysis oil. The degradation of lignin takes place at higher temperatures (200-450 °C) and is more complex than the decomposition of the previously mentioned substances. At the same time, free radicals are produced during the decomposition of lignin (Yaashikaa et al. 2020; Hu & Gholizadeh 2019).

In the primary phase, a solid carbonaceous residue and a condensable gas are formed. Condensable gas further decomposes into carbon monoxide, carbon dioxide, hydrogen, methane, and ethane. These non-condensable gases can be burned to generate the heat necessary for the pyrolysis process (Wallace et al. 2023).

3.7.3 Biochar from Sewage Sludge in relation to PFAS

The use of sewage sludge to produce biochar is a relatively new practice (Krahn et al. 2023). Sewage sludge itself may contain varying amounts of heavy metals, pathogens, microplastics, or organic contaminants including PFAS. PFAS can be released from contaminated sewage sludge during sludge treatment before pyrolysis (dewatering, drying of biosolids) or can be detected in pyrolysis products (biochar, pyrolysis gas, and oil) (Wallace et al. 2023). However, the resulting biochar from this potentially contaminated source has been found to contain lower levels of organic contaminants (including PFAS) and no pathogens (Thoma et al. 2022; Krahn et al. 2023). During pyrolysis at temperatures of 500-800 °C, more than 80% of 15 to 22 types of PFAS were removed from biochar and condensates. The exception was short-chain PFAS, which remained in pyrolysis products (Wallace et al. 2023). Thomas et al. (2022) reported a removal level of PFAS from biochar and condensates greater than 90%. Pyrolysis-treated sewage sludge can then be used to sorb toxic and bioaccumulative PFAS in soil (Wang et al. 2020a; Krahn et al. 2023). Stabilized sewage sludge that has not been pyrolyzed is not suitable for PFAS sorption in the soil. However, unlike biochar, it is a source of nitrogen (Thoma et al. 2022).

The process of removing PFAS from sewage sludge is not studied in detail and further research is needed, however, the basic mechanisms of this process are described (Thoma et al. 2022). As the temperature increases during pyrolysis, bonds between carbon atoms break first, followed by bonds between fluorine and carbon atoms. A mixture of volatile organofluorine compounds (e.g. tetrafluoroethylene, difluorocarbene, trifluoromethyl radicals, 1H-perfluoroalkanes, and perfluoroolefins) transitions into the gas phase. These substances can become part of the syngas or can be absorbed into solid particles (Thoma et al. 2022; Wallace et al. 2023). At the same time, residues or transformed PFAS may remain in the solid fraction (biochar) (Thoma et al. 2022). Short PFAS such as PFBA and PFPeA may volatilize unchanged during the drying process or when pyrolysis is initiated or terminated (Wallace et al. 2023).

According to Krahn et al. (2023), the sorption surface (expressed by the volume and the internal surface of the pores) of sludge biochar is smaller than for wood biochar. However, sludge biochar had more pores in the size range suitable for sorbing branched PFCA molecules compared to wood biochar. Despite the more optimal pore size distribution of sludge biochar, its effectiveness in the soil can be reduced by soil particles that block the pores. Large organic acids and humic substances in soils rich in organic matter have a similar effect. Reduced sorption capacity to sludge biochar was also demonstrated when contaminated with PFCA mixtures.

The utilization of sewage sludge in biochar production represents the economic and ecological management of this waste, resulting in a product with a wide range of applications. Nevertheless, it has been shown that not all PFAS can be absorbed equally effectively by biochar from sewage sludge. Short-chain PFCA, i.e. PFPeA, PFH_xA, and perfluoroheptanoic acid (PFHpA), which now represent an increasing threat to the environment, were poorly sorbed onto biochar. The reason for the poorer sorption of shorter PFCA on biochar may be the lack of sites for ion exchange. Ionic interactions may predominate with these short molecules over the hydrophobic interactions observed with longer PFCAs (Krahn et al. 2023).

3.7.4 Biochar from timber waste as a sorbent of PFAS

Biochar produced from wood biomass can be used for the sorption of PFAS (or organic micropollutants in general) in water and soil (Askeland et al. 2020; Hagemann et al. 2020; Sørmo et al. 2021). The effectiveness of wood biochar in sorbing organic micropollutants (anticorrosives, drugs, biocide) in wastewater was investigated by Hagemann et al. (2020). Micropollutants contained in the water were eliminated after the addition of wood biochar. The application of wood biochar to soil reduced the leaching of selected PFAS from the soil (Askeland et al. 2020; Sørmo et al. 2021). However, the effectiveness of biochar varies depending on the characteristics of the biochar, type of congener, and soil properties (Askeland et al. 2020).

The specific surface area of biochar can be influenced by the pyrolysis temperatures, just as in the case of sewage biochar. At temperatures of 500–600 °C, the pyrolyzed material had a smaller specific surface area (130–280 m² g⁻¹) and larger pores (pores > 1.5 nm) than the same material pyrolyzed at higher temperatures (specific surface area: 450–525 m² g⁻¹, pore size 0.3–1.5 nm) (Sørmo et al. 2021).

Steam, CO₂, and/or air activation also affect the size of the specific biochar surface (Hagemann et al. 2020). Activation is a process that creates new nanopores (<2 nm), resulting in an increase in the specific surface area of the biochar (Sørmo et al. 2021). According to Hagemann et al. (2020), this activation played a greater role in PFAS sorption than the quality of pyrolyzed wood.

As with sludge biochar, PFAS with a shorter chain (3 to 4 carbon atoms per molecule) is more difficult to sorb onto the surface of wood biochar compared to PFAS with 5 or more carbon atoms per molecule (Sørmo et al. 2021). This happens based on the electrostatic repulsion of negatively charged PFAS from negatively charged or polar oxygen-containing functional groups on the surface of the biochar. However, for PFAS with a longer chain, hydrophobic interactions prevail during sorption, and therefore they can be more efficiently

sorbed on the surface of biochar (Hagemann et al. 2020; Sørmo et al. 2021). Apart from the chain length, the functional group of the PFAS molecule also affects the sorption of biochar. Sørmo et al. (2021) observed stronger sorption of PFBS on wood biochar compared to PFPeAf with one carbon atom longer chain. However, the influence of the functional group on the sorption of PFAS with longer chains was not apparent. Askeland et al. (2020) also observed differential sorption of PFSA and PFCA onto wood biochar. PFHxS with 6 carbon atoms in the backbone chain was more strongly sorbed onto biochar in the soil compared to PFOA with 8 carbon atoms in the chain.

The effectiveness of wood biochar also depends on the properties of the soil to which it is applied. The sorption of PFAS is influenced by specific fractions of organic matter, such as carbohydrates, proteins, fulvic acids, and humic acids (Askeland et al. 2020). In soils with a lower TOC content, PFAS leaching was significantly reduced after the application of biochar compared to soils with a higher TOC content. In soils with a higher organic matter content, as in the case of sludge biochar, the pores were clogged with soil organic molecules. At the same time, soils with high TOC strongly sorb PFAS themselves. To overcome this soil sorption and prevent the leaching of PFAS, a higher dose of biochar is needed than in soils with low TOC content. In soils with low TOC, a 0.5% dose of biochar reduced PFAS leaching by more than 90%. Increasing the biochar dose further reduced the leachability of PFAS (Askeland et al. 2020; Sørmo et al. 2021). In soils with high TOC, leaching was reduced by a maximum of 60% with a biochar dose of up to 5% (Sørmo et al. 2021).

3.8 PFAS in the human organism

For a long time, global PFAS contamination went undetected. The first study pointing to the presence of fluorine in organic forms in human serum appeared in 1968. Since then, long-chain PFAS, including PFOA and PFOS, have been subject to observation and research (Munoz et al. 2019). Since 2000, PFOS, like other long-chain PFAS, has been phased out due to toxicity and accumulation in the environment (Bao et al. 2017).

People are exposed to toxic, persistent, and bioaccumulative (Bao et al. 2017; Munoz et al. 2019; Wang et al. 2020a) PFAS mainly by consuming contaminated food or through contaminated water (Munoz et al. 2019; Mei et al. 2021; Kancharla et al. 2022), further through contaminated indoor air and dust (Mei et al. 2021). PFAS can also get into food, and then into people, through food packaging (pizza boxes, popcorn bags), food packaging paper, or when using dishes (nonstick cookware) (Kancharla et al. 2022). In the human body, PFAS have been found in the blood, liver, and kidneys (Bao et al. 2017; Ghisi et al. 2019; Kancharla et al. 2022). The half-life of PFOA and PFOS in the liver is an average of 3.8 years for PFOA and 5.4 years for PFOS (Ghisi et al. 2019). F-53B substitute has the longest half-life (15.3 years) of all PFAS (He et al. 2022).

Studies investigating the toxicity of PFAS (mainly PFOA and PFOS) rely on experiments on laboratory animals, as human studies have not produced clear results (Ghisi et al. 2019). PFAS can act as endocrine and metabolic disruptors in humans, they can increase cholesterol levels (Cousins et al. 2020), cause thyroid gland dysfunction, immune response suppression, kidney disease, neurodevelopmental problems, and cardiovascular disease (Wang et al. 2020a; Kancharla et al. 2022) and cancer (Cousins et al. 2020; Wang et al. 2020a; Kancharla et al.

2022). In 2017, PFOA was classified by the International Agency for Research on Cancer as a potential human carcinogen causing kidney and testicular cancer (Xu et al. 2022). PFAS also has a negative effect on the lungs, and the reproductive system (Mei et al. 2021) and can damage the intestines and intestinal microflora (Gui et al. 2023). At the same time, PFAS can pass from mother to fetus through the umbilical cord (Ghisi et al. 2019). High placental permeability was observed in F-53B (He et al. 2022).

For PFAS with a shorter chain (perfluorobutanoic acid, perfluorohexanoic acid, perfluorobutane sulfonic acid), which serve as substitutes for PFOA and PFOS, the toxicity has not been investigated in detail (Ghisi et al. 2019). However, some studies suggest that shorter-chain PFAS are more toxic than the PFAS they replaced (Leung et al. 2023). An example is GenX, which according to the EPA is more toxic than PFOA, which this substance was supposed to advise. At the same time, there are indications that GenX may cause cancer after consumption (Kancharla et al. 2022). The toxicity of the OBS substitute has not been fully investigated, but it is believed to be as toxic and persistent as other PFAS. Therefore, the spread of this substitute in the environment and increased human exposure are of serious concern (Bao et al. 2017; Zhou et al. 2022). F-53B is considered moderately toxic based on preliminary studies (Xu et al. 2021).

3.9 Limits of PFAS in the environment

The increasing concentration of PFAS in the environment has brought with it limits for these substances. In 2008, the European Food Safety Authority (EFSA) set the acceptable weekly intake for PFOA at 1,500 ng/kg body weight and for PFOS at 150 ng/kg body weight. These limits have been tightened in the case of PFOS roughly 1,000 times in recent years and the case of PFOA almost 10,000 times. Acceptable weekly intake values are currently set for the sum of four selected PFAS accumulating in the human body (PFOA, PFOS, PFNA, PFHxS) and amount to 4.4 ng/kg of body weight (Kule et al. 2021).

The US Environmental Protection Agency (USEPA) drew attention to the presence of PFOS and PFOA in water. The concentration of PFOA and PFOS in the drinking water of more than 6 million US residents exceeded 70 ng/L, i.e. the health advisory level (Hopkins et al. 2018) (concentration at which adverse effects are not expected to occur during life) (EPA 2023d). Based on these findings, safe limits for PFAS in drinking water have been established. On WHO's recommendation, these limits were incorporated into the new Drinking Water Directive 2020/2184/EC (Hušková & Vojtěchovská Šrámková 2021). The limit for the total amount of PFAS is 500 ng/L of drinking water, for selected 20 PFAS the limit is set to 100 ng/L of drinking water (Hušková & Vojtěchovská Šrámková 2021; Kule et al. 2021). The selected PFAS include 10 C4-C13 perfluoroalkyl acids (PFBA - PFTrDA) and 10 C4-C13 perfluoroalkyl sulfonic acids (PFBS - PFTrDS). The limits from the European directive are gradually reflected in the Czech legislation. When amending Decree No. 252/2004 Coll. (hygienic requirements for drinking warm water) a limit of 100 ng/L for the sum of 20 PFAS and a limit of 10 ng/L for the sum of PFOS, PFOA, PFNA, PFHxS was set (Kule et al. 2021).

4 Methodology

The experimental part of the thesis consisted of a pot experiment and subsequent laboratory analyses of the biomass samples. The pot experiment was carried out in the outdoor precipitation-controlled vegetation hall of the Department of Agro-Environmental Chemistry and Plant Nutrition located in the university campus in Prague, Czech Republic. In the vegetation hall, the plants were protected from the precipitation water, had natural sunlight, and the temperatures were of natural ambient temperature. The cultivated plants were *Cucurbita pepo* L., a variety of zucchini. A total of 90 zucchini plants were grown on agricultural soil originating from vicinity of Humpolec city, Czech Republic. The soil collection site is located at an altitude of 527 m above sea level. The average annual precipitation is 603 mm, and the average temperature is 7.1 °C. The values of the basic parameters characterizing the soil are shown in Table 4.

Table 4: Basic characteristics of the soil in the pot experiment (Mercl et al. 2016; Ocheцова 2016).

Soil characteristics	Values
Soil type	Cambisol
Soil texture	Loam
pH _{H2O}	5.2 ± 0.1
Cation exchange capacity (mmol kg ⁻¹)	121 ± 2
Total C (%)	1.6 ± 0
Total N (%)	0.15 ± 0
Available P _{Mehlich 3}	99 ± 2

Wood biochar (WBC) was mixed with the soil in 30 flowerpots, sludge biochar (SSBC) was mixed with the soil in another 30 flowerpots, and the remaining 30 flowerpots served as a control. Sludge biochar was produced at a temperature of 600 °C using the Pyreg technology, which is installed at the Wastewater treatment plant in Bohuslavice – Trutnov, Czech Republic. Wood biochar is produced by ENERGO Zlatá Olešnice s.r.o. from waste wood chips at a temperature of 300–600 °C. Cultivated plants were irrigated with PFAS, PPCP, and PFAS+PPCP solutions. This thesis works only with data from plants irrigated with a solution of PFAS and a control treatment (methanol added instead of PFAS standard). There are 30 plants in total, each group counted 5 repetitions. The scheme of the experiment is shown in Table 5.

Table 5: Scheme of the pot experiment.

	Tap water	PFAS
Control	1-5	16-20
Control + SSBC	6-10	21-25
Control + WBC	11-15	26-30

The table represents the scheme of the experiment described in this thesis. Plants No. 1-15 were watered with a methanol solution (control treatment), and plants No. 16-30 were

watered with a PFAS solution. Both groups were further divided according to variants, which always included 5 flowerpots. Flowerpots No. 1-5 (watered with control treatment) and 16-20 (watered with PFAS solution) were designated as control, flowerpots 6-10 (watered with control treatment) and 21-25 (watered with PFAS solution) were designated as control + SSBC, and flowerpots No. 11-15 (watered with control treatment) and 26-30 (watered with PFAS solution) were designated as control + WBC.

4.1 Preparation of an outdoor experiment

The pot experiment was established between June 13 and 14, 2023. On the first day, 90 flowerpots with a volume of 1.5 kg of soil were prepared. The flowerpots and saucers were cleaned with ethanol before use. 1.3 kg of soil was calculated for each flowerpot. The weight of the soil was chosen to allow efficient water inflow and to prevent the creation of an undesirable microclimate supporting the formation of molds. In total, 150 kg of soil (Cambisol loam) was used. The soil was homogenized and divided into 3 equal segments of 50 kg each. 250 g of limestone and 286 ml of NPK fertilizer were added to each segment. Fertilizer parameters are listed in Table 6.

Table 6: Parameters of the NPK fertilizer used in establishing the pot experiment.

A sign of quality	Value [%]	The amount of applied nutrients [mg/kg]
Total nitrogen as N	7.0	496.5
Ammonium nitrogen as N	5.0	354.64
Nitrate nitrogen as N	2.0	141.86
Phosphorus as P	3.06	216.78
Potassium as K	4.15	294.28
Sulfur as S	2.0	141.86
Zinc as Zn	0.005	0.35
Copper as Cu	0.005	0.35
Molybdenum as Mo	0.002	0.14
Iron as Fe	0.02	1.42
Manganese as Mn	0.01	0.71
Boron as B	0.01	0.71

One 50 kg segment enriched with limestone and fertilizer was left as a control, SSBC (261.5 g) and WBC (86.9 g) were added to the other two. The total weight of added biochar depended on the weight of biochar in one pot. It was determined that the biochar would occupy 0.5% of the weight in the flowerpot, i.e. 6.5 g. The resulting weight of biochar was further modified based on the moisture and C content values to achieve the same C content supplied by the biochar in each pot. Moisture content, C, H and N content, and H/C molar ratio, which were determined based on laboratory measurements, are shown in Table 7.

Table 7. Parameters of sludge and wood biochar used in the pot experiment.

	Sludge biochar	Wood biochar
Moisture [%]	5	13
C content [%]	27.48	90.76
H content [%]	1.35	0.94
N content [%]	3.19	0.22
H/C molar ratio	0.59	0.124
Applied amount of biochar [g/kg]	5.23	1.74

In variants 6-10, and 21-25 (see Table 4), 6.8 g of SSBC was added to 1.3 kg of soil, in variants 11-15, and 26-30 (see Table 4) an additional 2.26 g of WBC was added. In total, 261.5 g of SSBC was added to one 50 kg part of the soil, and 86.9 g of WBC to the other. The soil was homogenized again after the addition of biochar. After filling the pots with soil, the pots were randomly distributed in the greenhouse to ensure equal conditions for all plants. Then the pots were randomized once a week.

On the second day, i.e. 14/06/2023, 2 zucchini seeds were planted in each pot, and 0.1 g of diatomaceous earth was applied to them. The diatomaceous powder was added as a control because the experiment consisted of arbuscular mycorrhizal fungi treatment but that was not part of this thesis. Then the seeds were covered with soil, and the soil was pressed.



Figure 4: Zucchini seeds with diatomaceous earth applied before covering with soil (own photo documentation).

4.2 Irrigation

Plants were initially watered to 60 % water capacity. This value was chosen as an optimal compromise between the amount of water and air in the pores needed for plant emergence. In

the middle of the experiment, this value was raised to 75 %, because at 60 % filling of the pores with water, the plants tended to dry up very fast. From the establishment of the experiment until 29/06/2023, the plants were irrigated with tap water, and then, when number of emerged plants per pot was reduced to one, prepared solutions of contaminants were used for irrigation. Then plants 1-15 were irrigated with the control solution, and plants 16-30 were irrigated with the PFAS solution.

4.3 Preparation of chemicals

Before each watering, the appropriate contaminant solutions were prepared from the stock solution. During the preparation of the solutions and the subsequent watering, care was taken to avoid contamination of the plants with other contaminants (changing gloves and washing equipment with ethanol when changing variants). Samples were taken from each prepared solution into plastic bottles to determine the total concentration of contaminants that were added to the flowerpot.

4.3.1 Preparation of the stock solution

The stock solution was prepared as a solution of the substances HFPO-DA, HFPO-TA, HFPO-TeA, PFOA and PFOS and methanol in a 100 ml volumetric flask. The effort was to ensure a concentration of 10 ppm (10 mg/L) of each contaminant in the stock solution. The resulting volume of contaminants applied to the stock solution was modified based on contaminant purity, density, and molar mass. PFOA and PFOS as solids had to be dissolved in MeOH prior to preparing the stock solution. Similarly, liquid PFAS (HFPO-DA, HFPO-TA, and HFPO-TeA) were firstly 100x diluted by MeOH and then used for the stock solution preparation.

4.3.2 Preparation of the irrigation solution

The irrigation solutions were prepared in 2l volumetric flasks with a contaminant concentration of 1ml of stock solution per 1l of water resulting in the final concentration of 10 µg of each contaminant per liter of irrigation water. In total, 2 ml of methanol stock solution (control) and PFAS were pipetted into the volumetric flask. Contaminants were pipetted into a small amount of water in a volumetric flask. Subsequently, the volumetric flasks were topped up to the mark with tap water, closed, and shaken. The resulting amount of water was measured in a volumetric cylinder. All plants were supplied with the same amount of chemicals.

4.4 Harvest

The harvest took place on August 9, 2023 after 57 days of plant growth (plants during growth are shown in Figures 5, 6, 7).



Figure 5: Plants after 14 days of growth, photographed on 6/28/2023 (own photo documentation).



Figure 6: Plants after 44 days of growth, photographed on 28/7/2023 (own photo documentation).



Figure 7: Zucchini fruit after 57 days of plant growth, photographed on 9/8/2023 (photo by Sreynet Nang).

During harvesting, great care was taken to prevent contamination of the plants with other contaminants. All tools were regularly washed with methanol. The above-ground biomass of the plants was cut off and divided into fruit and vegetative organs. The fruits were sliced, the above-ground biomass was cut, and everything was weighed and wrapped in aluminum foil (Figure 8). The roots were removed from the soil, washed in tap water, and stored in PP tubes (50 ml). Parts of the plants were stored in liquid nitrogen in the greenhouse. Subsequently, the samples were transported to the laboratory and frozen at a temperature of -80°C .



Figure 8: Cut above-ground biomass of zucchini on a scale (own photo documentation).

4.5 Laboratory part of the experiment

Zucchini fruits were lyophilized (Figure 9) and then crushed in a ceramic mortar (cleaned with methanol) using liquid nitrogen (Figure 10). Before further analysis, samples were stored in a freezer at -20°C . The lyophilized and crushed samples were first extracted using the QuEChERS (Quick, Easy, Cheap, Effective, Rugged and Safe) method. To 0.1 g of crushed lyophilized sample in tubes (15 ml), internal standard solution of isotopically labelled analogues was added, sample was vortexed and then 2 ml of Milli-Q water was added. The samples were vortexed and stored for 10 minutes in a refrigerator (temperature 4°C). After removal from the refrigerator, 1 ml of acetonitrile (MeCN) was added to all samples, followed by vortexing for 1 minute. Then, the samples were placed in the Elma S 100 H Elmasonic sonicator for 5 minutes (Figure 11). After removal from the sonicator, 0.65 g of QuEChERS salt (4 g MgSO_4 , 1 g NaCl , 1 g Trisodium Citrate Dihydrate, 0.5 g Disodium Hydrogenecitrate Sesquihydrate) was added to the samples. These samples were then vortexed for 1 minute and placed in an Ohaus Frontier 5718R centrifuge for 10 minutes at a temperature of 4°C and a speed of 2490 g. After removal from the centrifuge, the supernatant was transferred using a Pasteur pipette to a 1.5 ml Eppendorf tube. From there, 700 μl of the supernatant was transferred with a micropipette into Eppendorf tubes containing 150 mg MgSO_4 , 50 mg PSA (primary secondary amine), and 20 mg GCB (graphite carbon black). The samples were vortexed again and placed in a centrifuge for 10 minutes at a temperature of 4°C and a speed of 24104 g (Figure 12). After removing the samples from the centrifuge, 400 μl of the supernatant was transferred to LC/MS vials by

Pasteur pipetting and was submitted to LC-MS/MS analysis using Agilent 6495B triple quadrupole mass spectrometer.



Figure 9: Lyophilization of zucchini samples (own photo documentation).



Figure 10: Grinding zucchini fruits in a ceramic mortar (own photo documentation).



Figure 11: Supernatant samples placed in the sonicator (own photo documentation).



Figure 12: Supernatant samples placed in the centrifuge (own photo documentation).

4.6 Statistical data processing

One-way ANOVA in the Statistica 12 program was used to evaluate the data obtained from LC/MS. The soil variant (control, soil with WBC, and soil with SSBC) was chosen as a factor. Data normality was tested using the Shapiro-Wilk test, and differences between variants were then analyzed using the post hoc Tuckey HSD test. Results were considered statistically significant at $p < 0.05$. In the Statistica program, the dependence of PFAS concentration on the weight of zucchini fruits was evaluated using regression analysis. The MS Excel program was used for the graphical presentation of the results.

A distribution factor was calculated from the data on the amount of contaminants in the fruits (Equation 3). It is a percentage that represents the proportion of a given contaminant in the fruit to the total amount of contaminants applied to the plant (Equation 4).

$$\text{Amount of contaminant [ng]} = \text{concentration [ng/g]} * \text{yield [g]} \quad (3)$$

$$\text{Distribution factor [\%]} = (\text{amount of contaminant} * 100) / \text{total amount of chemicals applied to each pot [ng]} \quad (4)$$

For plant No. 30, which had 2 fruits, the measured amounts of contaminants in both fruits were summed and subsequently presented as the resulting amount of contaminants for the given plant. This value was subsequently treated as the other values obtained for plants with 1 fruit.

5 Results

5.1 Yield of fresh and dried fruit biomass

During watering, each plant was irrigated with 7.815 L of contaminated water. The concentration of each contaminant in this water was 10 µg/L. Thus, a total of 78.15 µg of each contaminant (HFPO-DA, HFPO-TA, HFPO-TeA, PFOA, PFOS) was added to each plant.

The average fresh fruit biomass weights with standard deviations are shown in Figure 13. The average dry fruit biomass weights with standard deviations are shown in Table 8. The weights of fresh and dry biomass for all plants are shown in Appendix 1. For each plant from variants 1-30, except for plants No. 4 and 24, the fruit was weighed in a fresh and dry state. Plant No. 4 did not grow, plant No. 24 had no fruit. In the case of plants with 2 fruits (plants No. 3, 5, 6, 9, 11, 14, and 30), the weight of both fruits was summed and presented as fruit weight/pot. Plant No. 4 did not grow, plant No. 24 had no fruit. The values were statistically evaluated, then averaged under the variants (control, control SSBC, control WBC, PFAS, PFAS SSBC, PFAS WBC), and converted into a graphic form.

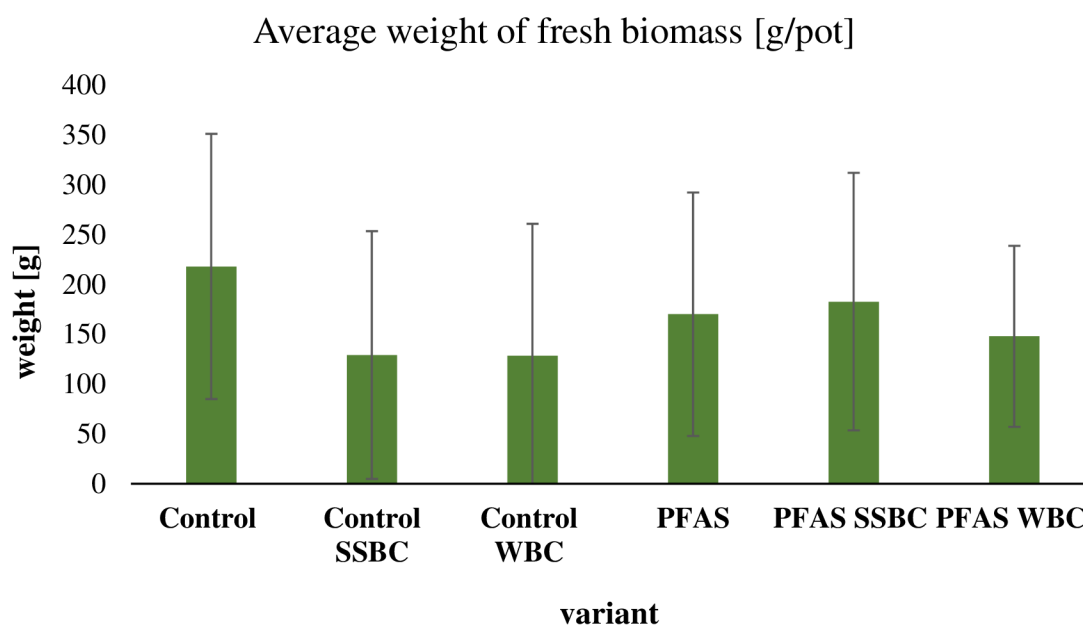


Figure 13: Average weight of fresh biomass with standard deviations by variants.

Table 8: Average weight of dry biomass according to variants.

variety	control	control SSBC	control WBC	PFAS	PFAS SSBC	PFAS WBC
weight of dry biomass [g]	16.23 ± 12.81	7.47 ± 6.45	6.51 ± 5.68	9.71 ± 5.85	9.79 ± 6.82	7.73 ± 4.05

After statistical evaluation of the data (fruit weight/pot) in the Statistica program, it was found that there was no statistically significant difference between the weights between the variants (p-values were higher than 0.05).

It can be seen from Figure 13 that the largest average weight of fresh biomass was in Control (272.28 g), even though plant No. 4 did not grow. This increase in weight may be due to plants with two fruits (plant No. 3 and 5). The smallest average weight of fresh biomass was found for the variant Control WBC (128.12 g) and Control SBC (128.98 g), even though plants No. 6, 9 (variant control SSBC), 11, 14 (variant control WBC) had 2 fruits. The same trend can be observed for dry biomass. The highest average dry biomass weight was observed in the Control variant (16.23 g), and the lowest in the Control WBC variant (6.51 g).

5.2 The effect of biochar on the amount of PFAS in fruits

The averaged concentration values in dry biomass, are shown together with the standard deviations in Table 9. In Table 9, the averaged values of the concentration of PFAS in fresh biomass for the given variants are also shown with the standard deviations. The concentrations in dry biomass and fresh biomass obtained from individual plants are shown in Appendix 2. Measurable concentrations of contaminants were found only in plants treated with PFAS solutions, i.e. in plants no. 16-30. Contaminant concentrations in variants irrigated with the control solution (plants No. 1-15) were below the LC/MS detection limit. Concentration values were obtained from LC/MS in pg/ml and subsequently converted to ng/g. In the case of plant No. 30, which had 2 fruits, the concentration of both fruits was summed and presented as the resulting contaminant concentration per sum of fruits. The resulting mean contaminant amounts with standard deviations measured for the 3 variants are shown for HFPO-DA in Figure 14, for HFPO-TA in Figure 15, for HFPO-TeA in Figure 16, for PFOA in Figure 17 and for PFOS in Figure 18. The measured amounts of contaminants for each plant are shown in Appendix 3. The total amount of contaminants in zucchini fruits was calculated as the product of the contaminant concentration in the fruit [ng/g] and the total amount of dry biomass [g].

Table 9: Average contaminant concentration values with standard deviations in zucchini fruits according to variants.

Variant	HFPO-DA	HFPO-TA	HFPO-TeA	PFOA	PFOS
	[ng/g dry biomass]				
PFAS	23.41 ± 8.35	0.1 ± 0.1	<MLOD	7.23 ± 3.76	0.73 ± 0.28
PFAS SSSBC	14.37 ± 11.7	0.26 ± 0.24	0.16 ± 0.28	5.63 ± 4.72	0.64 ± 0.43
PFAS WBC	32.86 ± 16.73	0.31 ± 0.41	<MLOD	9.53 ± 8.04	0.96 ± 0.58
Variant	[ng/g fresh biomass]				
PFAS	1.51 ± 0.62	0.01 ± 0.01	<MLOD	0.45 ± 0.21	0.05 ± 0.02
PFAS SSSBC	0.77 ± 0.66	0.02 ± 0.01	0.01 ± 0.02	0.31 ± 0.29	0.04 ± 0.02
PFAS WBC	1.87 ± 0.86	0.02 ± 0.02	<MLOD	0.52 ± 0.4	0.05 ± 0.03

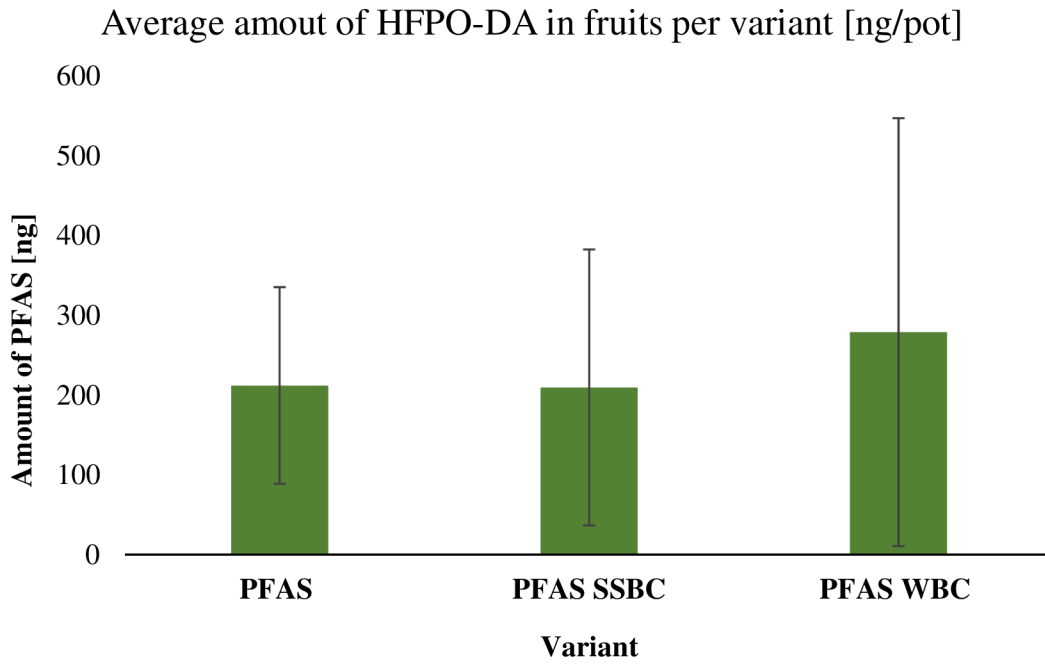


Figure 14: Average amount of HFPO-DA with standard deviations by variant.

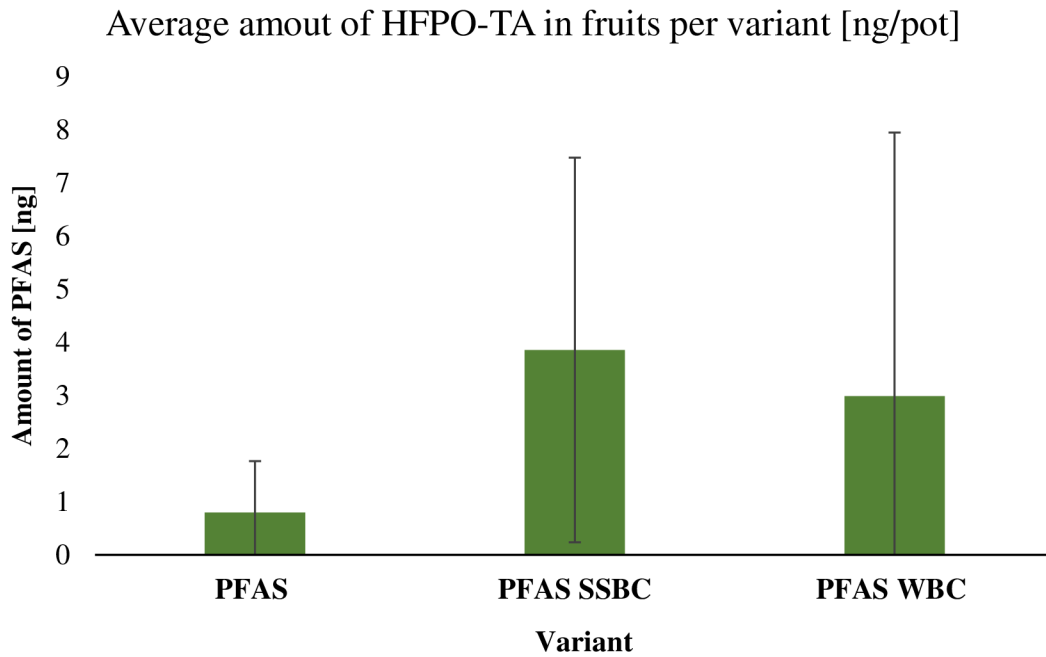


Figure 15: Average amount of HFPO-TA with standard deviations by variant.

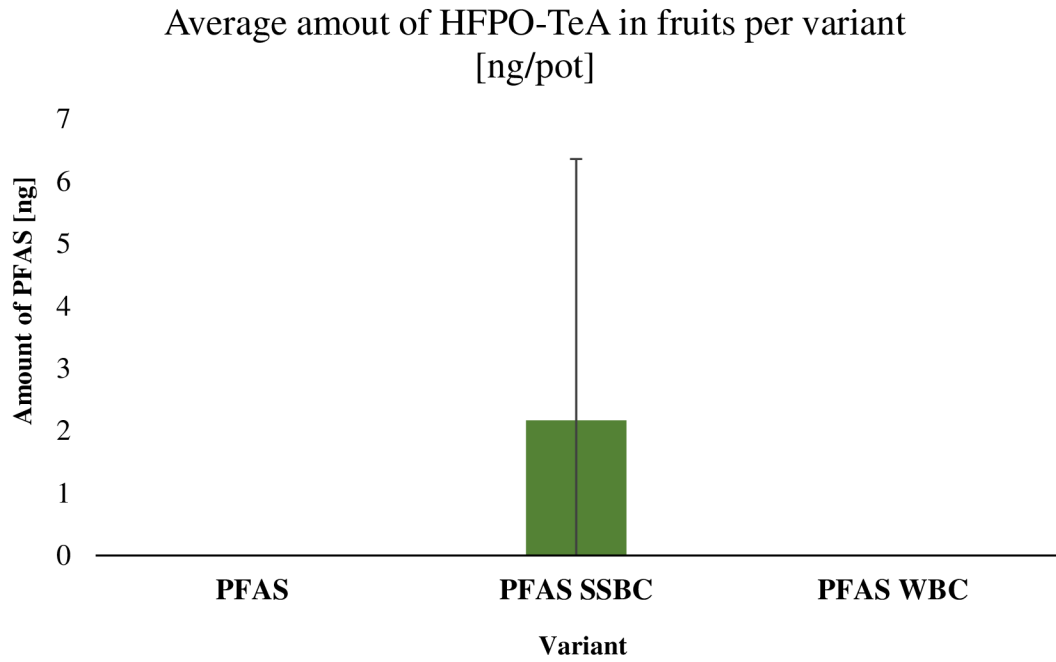


Figure 16: Average amount of HFPO-TeA with standard deviations by variant.

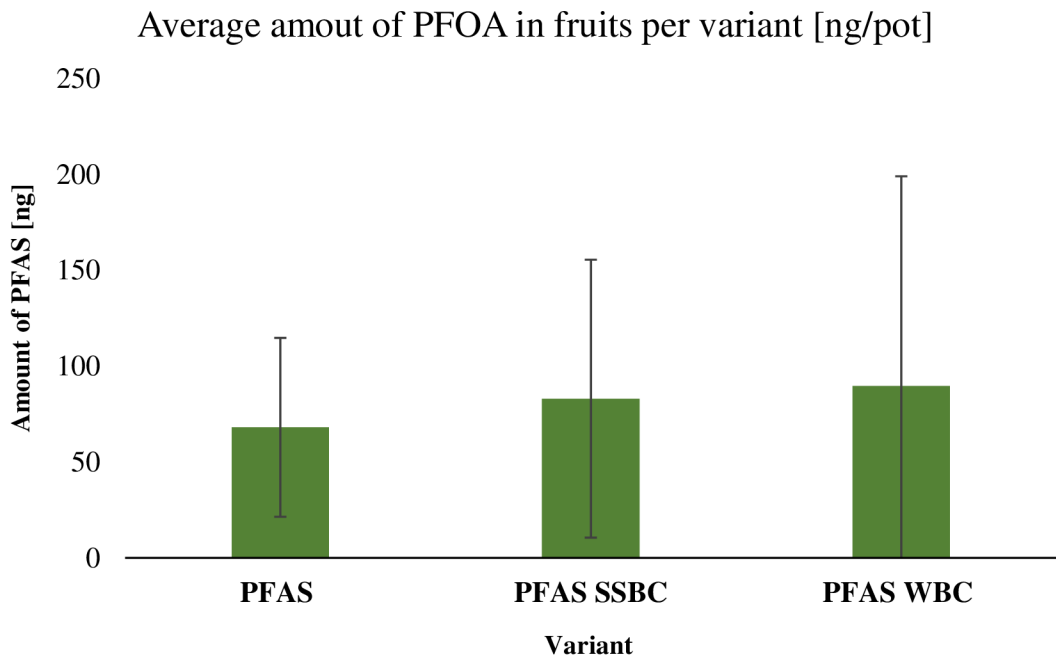


Figure 17: Average amount of PFOA with standard deviations by variant.

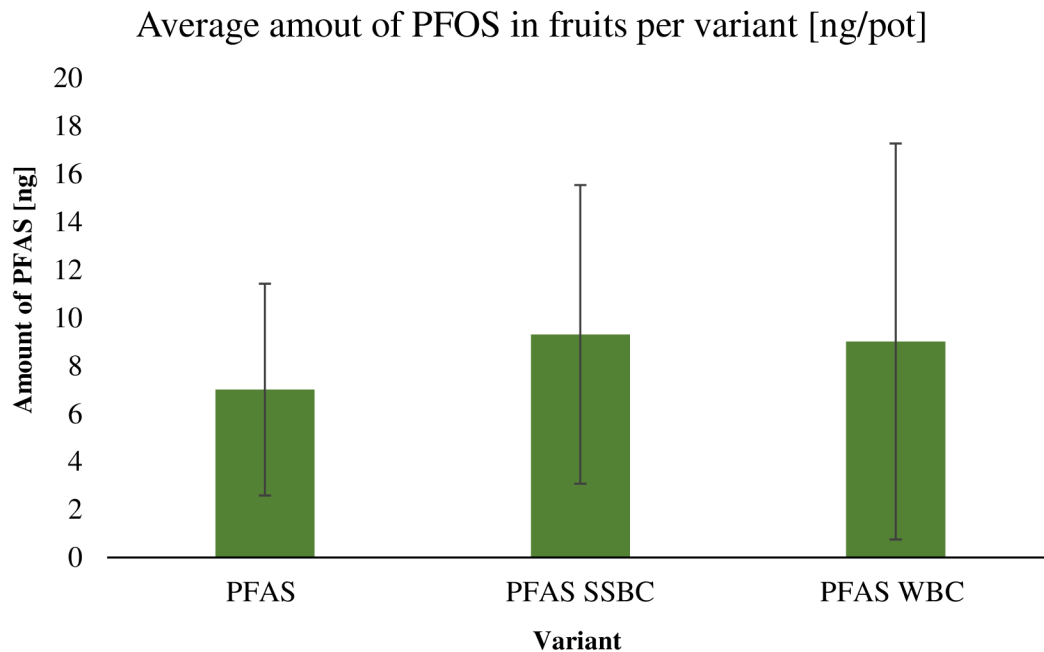


Figure 18: Average amount of PFOS with standard deviations by variant.

After statistical evaluation of the contaminant concentration [ng/g] in the Statistica program, it was found that no statistically significant difference between the variants was found for any contaminant (p-values were higher than 0.05).

From the graphs in Figures 14-18, it can be seen that the highest average amount of contaminant was measured for HFPO-DA in all variants (Figure 14), with the highest amount observed in the PFAS WBC variant (278.92 ± 286.2 ng). The second highest average amounts of contaminants were measured for PFOA (Figure 17) in all variants, with the highest amount observed in the PFAS WBC variant (89.63 ± 109.34 ng). The smallest amount of contaminant was measured in the case of HFPO-TeA (Figure 16) in the PFAS and PFAS WBC variants. The measured contaminant concentrations, from which the average amount of contaminants per given variant was subsequently calculated, were below the LC/MS detection limit for all plants in both variants. The second smallest amount of contaminant was measured for HFPO-TA (Figure 15) in the PFAS variant (0.8 ± 0.97 ng), where HFPO-TA concentrations below the detection limit of LC/MS were measured in plants No. 17 and 20. The third lowest amount of contaminant was measured for HFPO-TeA (Figure 16) in the PFAS SSBC variant (2.17 ± 4.2 ng). In this variant, the concentrations from which the amount of HFPO-TeA was subsequently calculated were found only in 2 plants (No. 23, 25). In the remaining plants, the concentration was below the detection limit of LC/MS.

Furthermore, it can be seen from the graphs in Figure 14-18 that the highest average amounts of HFPO-DA (278.92 ng) (Figure 14) and PFOA (89.63 ng) (Figure 17) were found in fruits grown on the variant with WBC, while in the case of HFPO-TA (3.85 ng) (Figure 15), HFPO-TeA (2.17 ng) (Figure 16) and PFOS (9.31 ng) (Figure 18), the greatest amount of contaminants were found in fruits grown on the variant with SSBC. The SSBC variant showed

higher concentrations of HFPO-TA and PFOS even though plant No. 24 did not grow, and plant No. 23 had concentrations below the LC/MS detection limit.

5.3 The relationship between the weight of zucchini and the total amount of contaminants

The dependence of the amount of contaminants [ng] on the mass of dry biomass [g] is shown for HFPO-DA in Figure 19, for HFPO-TA in Figure 20, HFPO-TeA in Figure 21, PFOA in Figure 22, and PFOS in Figure 23.

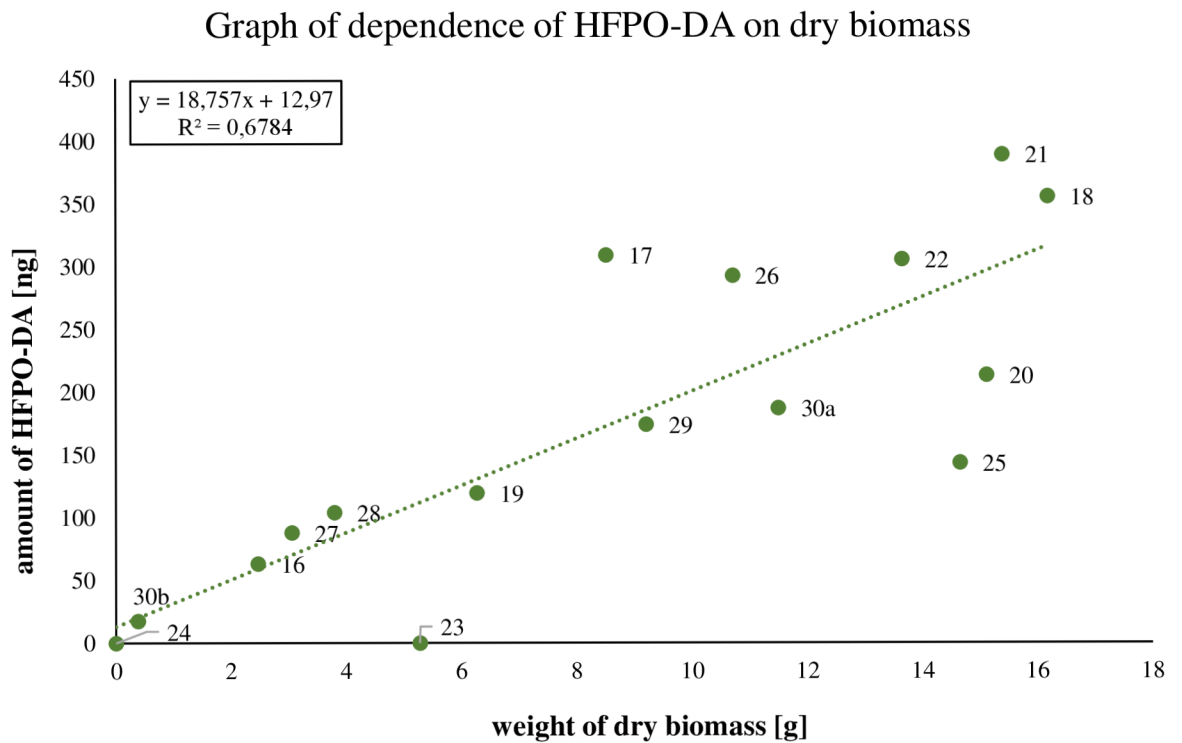


Figure 19: Graph of the dependence of the amount of HFPO-DA [ng] on the weight of dry biomass [g].

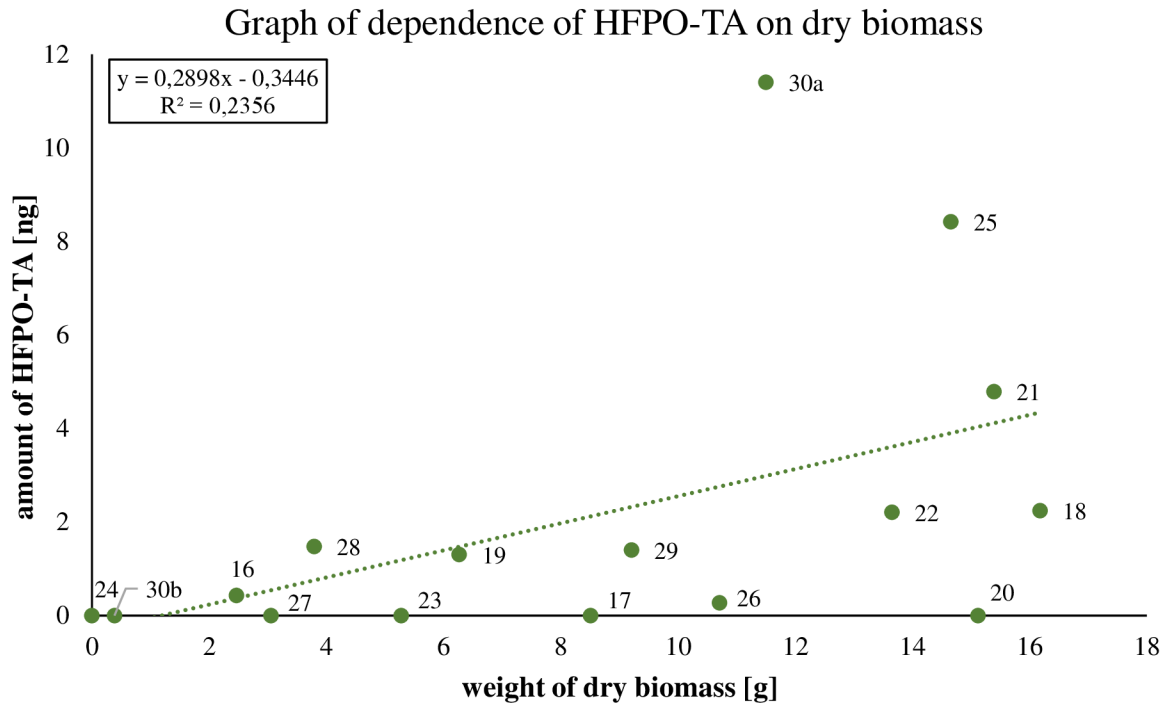


Figure 20: Graph of the dependence of the amount of HFPO-TA [ng] on the weight of dry biomass [g].

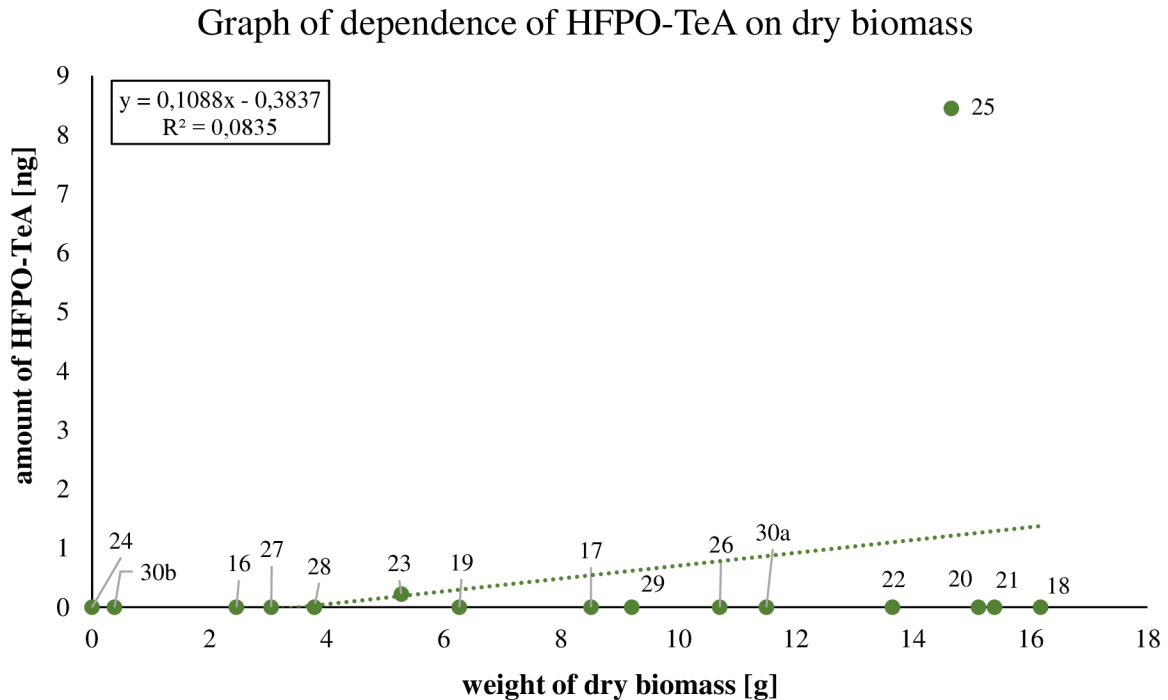


Figure 21: Graph of the dependence of the amount of HFPO-TeA [ng] on the weight of dry biomass [g].

Graph of dependence of PFOA on dry biomass

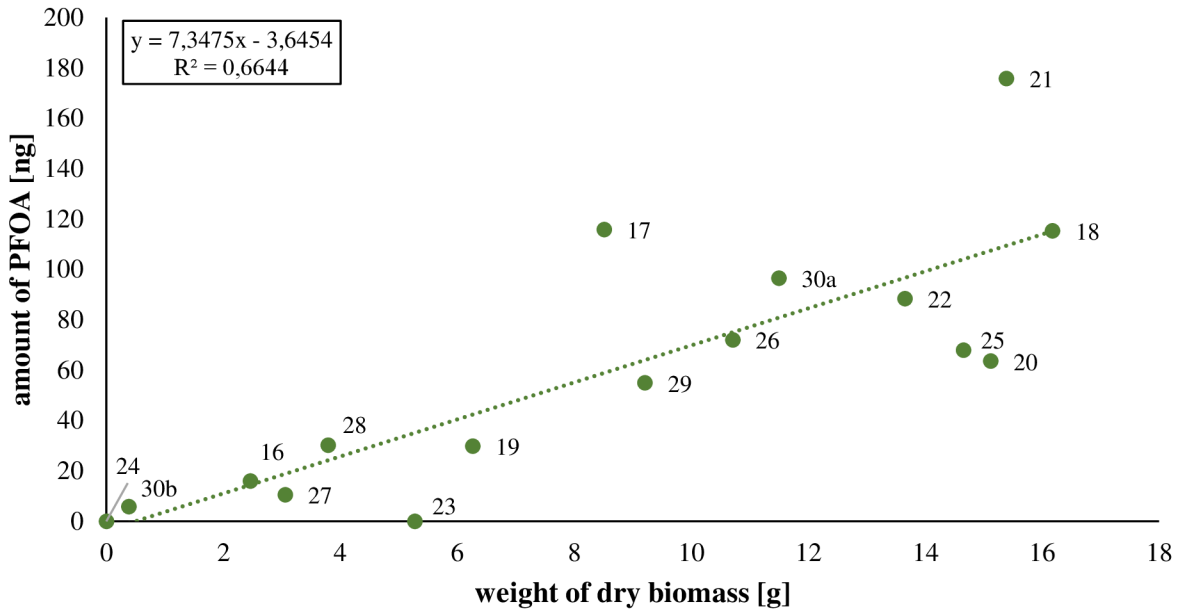


Figure 22: Graph of the dependence of the amount of PFOA [ng] on the weight of dry biomass [g].

Graph of dependence of PFOS on dry biomass

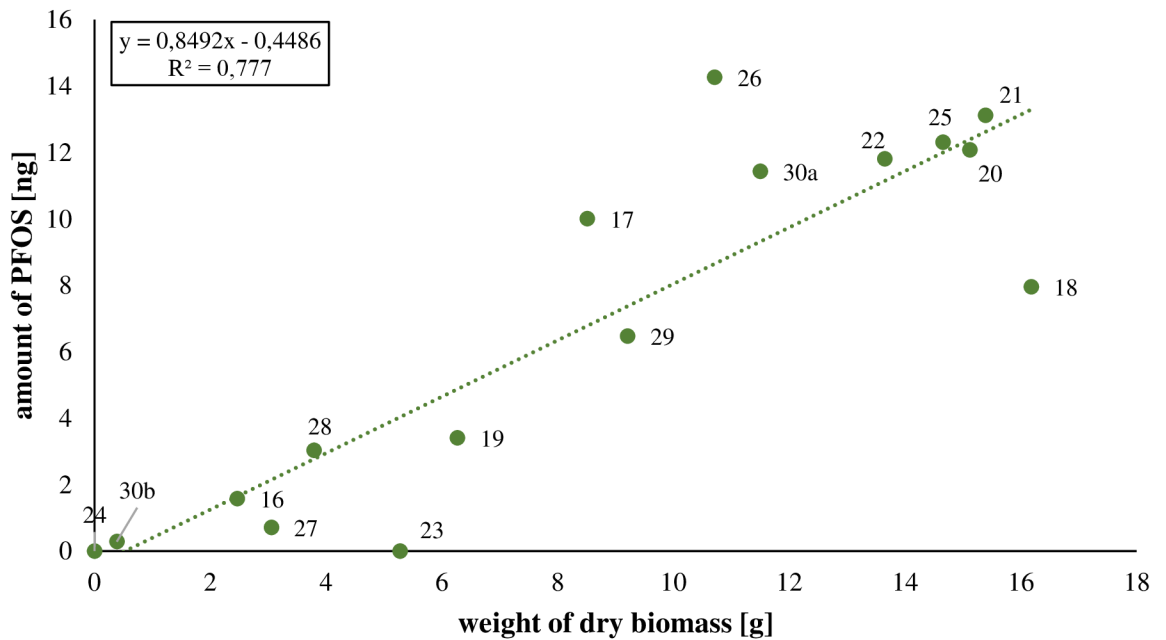


Figure 23: Graph of the dependence of the amount of PFOS [ng] on the weight of dry biomass [g].

Regression and correlation analysis in the Statistica program was used to evaluate the dependence between the amount of contaminant and the weight of dry biomass. From the obtained data, it is evident that a statistically significant dependence between the amount of contaminant and the weight of dry biomass was observed in the case of HFPO-DA, PFOA, and PFOS (p-values were lower than 0.05). In all three cases, the value of R (Pearson's correlation coefficient) was greater than 0.6 ($R_{\text{HFPO-DA}}=0.82$, $R_{\text{PFOA}}=0.82$, $R_{\text{PFOS}}=0.88$), and therefore there is a strong dependence between the mass of dry biomass and the amount of contaminants. R values and p values are shown in Table 10. As the weight of the dry biomass of the fruits increased, so did the amount of contained contaminants (linear direct dependence).

Table 10. P values and R values for contaminants statistically dependent on fruit dry biomass weight

Contaminant	p values	R values
HFPO-DA	0.00	0.82
PFOA	0.00	0.82
PFOS	0.00	0.88

Among the fruits with the highest dry biomass weight, and therefore the highest, or one of the highest, amounts of contaminants, are fruits from plants 18, 20 (PFAS variant), 21, 22, and 25 (PFAS SSBC variant). The highest amounts of HFPO-DA (389.1 ng) and PFOA (175.9 ng) of all replicates were measured in plant No. 21. In the case of PFOS, the second highest amount of contaminant was measured in plant No. 21 (13.12 ng) after plant No. 26 (14.26 ng).

According to the graph in Figure 20, plants 18, 21, 22, and 25 also contained high values of HFPO-TA, although for this contaminant no statistically significant dependence between its amount and the weight of dry biomass was demonstrated.

Not only for HFPO-TA but also for HFPO-TeA, no statistically significant dependence between the mass of dry biomass and the amount of contaminant was found based on observations (p-values were higher than 0.05). This fact is also evident from the graphs in Figures 20 and 21. In the case of HFPO-TeA, measurable concentrations of the contaminant were found only in plants No. 23 (0.22 ng) and 25 (8.45 ng) in the PFAS SSBC variant. In the remaining plants, the concentrations of the contaminant were below the limit of LC/MS detection. For HFPO-TA, undetectable concentration was found in plants 17, 20, 23, 24, 27, and 30b. In the remaining plants, the amount of HFPO-TA ranged from 0.27 ng (plant No. 26) to 11.41 ng (plant No. 30a).

5.4 Distribution factor

The average values of distribution factor for each variant are shown in Table 11. The values of the distribution factor for each plant are shown in Appendix 4.

Table 11: Average values of the distribution factor with standard deviations in individual variants.

Variant	Uptake of HFPO-DA	Uptake of HFPO-TA	Uptake of HFPO-TeA	Uptake of PFOA	Uptake of PFOS
	[%]				
PFAS	0.271±0.158	0.001±0.001	<MLOD	0.087±0.06	0.009±0.006
PFAS SSBC	0.268±0.221	0.005±0.005	0.003±0.005	0.106±0.093	0.012±0.008
PFAS WBC	0.221±0.106	0.004±0.006	<MLOD	0.069±0.046	0.009±0.007

It can be seen from Table 11 that the highest values of the distribution factor were observed in all variants for HFPO-DA, specifically in the PFAS variant (0.271%), followed by the PFAS SSBC variant (0.268%) and the PFAS WBC variant (0.221%). The second contaminant with the highest distribution factor value was PFOA. The highest distribution factor value for PFOA was recorded in the SSBC PFAS variant (0.106%), and the lowest in the WBC PFAS variant (0.069%). The smallest values of the distribution factor were recorded for the HFPO-TeA contaminant in the PFAS and PFAS WBC variants, as the amount of contaminants in the plants in these variants came out below the detection limit of LC/MS. Measurable values of the distribution factor were obtained for HFPO-TeA only in the PFAS variant SSBC (0.003%). Low values of the distribution factor were also recorded for HFPO-TA in all variants. The highest value of the distribution factor for HFPO-TA was recorded in the PFAS SSBC variant (0.005%), and the lowest in the PFAS variant (0.001%).

6 Discussion

6.1 Environmental relevance of PFAS concentration in water

The concentration of PFAS in water (10 µg/L) was determined in laboratory conditions, but it was based on data supported by professional literature. PFAS have been detected in waters all over the world in varying concentrations. Xu et al. (2021) investigated in their work the concentration of several PFAS including PFOA and PFOS at several locations in China, namely in surface and groundwater in rural areas in the east of the country (the average concentration of PFOA was 90.8 ng/L, 60 and less ng/L in other PFAS), near the drinking water reservoir Yuqiao Reservoir (average PFOA concentration 1.88 ng/L, average PFOS concentration 0.49 ng/L), in the Daling River Basin (average PFOA concentration 1421.6 ng/L, average PFOS concentration 0.4 ng/L) and Hutuo (average PFOA concentration 0.63 ng/L) and near a fluorochemical industrial plant (average PFOA concentration 1411.6 ng/L, average PFOS concentration 96.2 ng/L). Furthermore, PFAS concentrations were investigated in India in the Ganges River basin (average PFOA concentration 0.4 ng/L, average PFOS concentration 0.432 ng/L), in Australia in wells near the Melbourne landfill (average PFOS concentration 413 ng/L) or on an island Gozo (PFOA concentration 1.46 ng/L), which is part of the Maltese Islands. At all locations, PFOA and PFOS were detected in the range of tenths to thousands of ng/L. The concentrations of PFOA and PFOS in the water at the sampling sites were therefore lower than in the irrigation water in the pot experiment.

The concentration of GenX also came out in the range of tenths to hundreds of ng/L, i.e. again less than in the pot experiment. The concentration of GenX in the water near the fluorochemical plant near the city of Dordrecht in the Netherlands (average concentration of GenX 2.2 µg/L) and the water flowing out from the sewage treatment plant (average concentrations in the range of 134 to 375 µg/L) were investigated between 2006 and 2018 by Gebbink & van Leeuwen (2020). GenX was also found in the Rhine River at the Dutch-German border (0.75 ng/L) and in Germany (22 ng/L) or in the Nieuwe Waterweg River (concentration range 1.7 to 812 ng/L), but also in groundwater in the vicinity of the city of Dordrecht (concentrations in the range of 6–660 ng/L depending on the distance from the fluorochemical production plant). In Europe, however, it was found 300 places where the concentration of PFAS exceeded 10 µg/L. In Belgium, PFAS concentrations in the order of thousands of µg/L were even measured in the vicinity of a PFAS manufacturing site. High values were further measured for example in the Netherlands (Salvidge & Hosea 2023). High concentrations of PFAS, specifically GenX, have also been measured in the USA. In the Ohio River, a GenX concentration of 17.5 µg/L and higher was measured (Hopkins et al. 2018).

The contents of PFAS in water in the Czech Republic were addressed in their work by Dvorakova et al. (2023) and Salvidge & Hosea (2023). Dvorakova et al. (2023) monitored the concentration of sum PFAS in drinking water. A total of 192 drinking water samples were analyzed, in which 80% of PFOA was detected, less PFOS was detected. The concentration values of the sum of PFAS ranged from undetectable values to 23.9 ng/L. The PFAS concentration values reported by Salvidge & Hosea (2023) ranged from tens to hundreds of ng/L. Dvorakova et al. (2023) further mentioned in their work that the presence of PFAS in water in the Czech Republic is very low. This was also confirmed in the pot experiment. PFAS

were not detected in plants that were watered with tap water (control treatment), just as PFAS were not detected in some samples in the study by Dvorakova et al. (2023).

In no case did the measured values from the Czech Republic exceed the concentration value of 10 µg/L used in the pot experiment. However, it is evident from the literature that concentrations in the order of units to tens of µg/L are not unrealistic and that they can be found in waters across continents.

6.2 Effect of biochar and PFAS on fruit weight

6.2.1 Effect of biochar on fruit weight

It can be seen from the graph in Figure 13 that the mean weight of fresh fruit biomass differed between the variants, yet no statistically significant difference was observed between the variants. The highest average fruit weight was measured in the Control variant, i.e. watered with tap water and without the addition of biochar. The lowest average fruit weights were measured on the Control SSBC and Control WBC variants, even though these plants were also watered with tap water, but had biochar added to the soil.

The addition of biochar to the soil improves soil properties, which ultimately leads to higher plant yields. This trend was described in the work of Farhangi-Abriz et al. (2021), who recorded higher corn and wheat grain yields after applying biochar to the soil. Farid et al. (2022) observed increased yields in zucchini grown on arid soils after the addition of rice straw and sugarcane bagasse biochar. It could therefore be assumed that variants with applied biochar will have a higher yield compared to variants without biochar. In the pot experiment, however, a higher average fruit weight was recorded on the Control variant compared to the Control + biochar variants. Also, the average weight of fruits grown on the PFAS variant was higher than the average weight of fruits from the PFAS WBC variant, but at the same time, it was lower than the weight of fruits from PFAS SSBC variant. The reason for the different yields of zucchini fruits may be different input conditions (soil type, pyrolyzed material) in the pot experiment and the work of Farid et al. (2022). Brnicky et al. (2021) drew attention to the variability of the structure of biochar and its sorption capabilities even with a slight change in the pyrolyzed material or the pyrolysis process itself.

Another reason for the reduced yield may paradoxically be a decrease in available nutrients in the soil due to the high sorption potential of biochar, even though after the application of biochar there is an increase in the total content of nutrients (observed for nitrogen and phosphorus). This phenomenon, which negatively affects the yield of crops, was described again in their work by Brnicky et al. (2021). He further pointed out the relationship between the yield and the content and availability of nutrients in the biochar itself. The amount of nutrients and the ability to release them into the surrounding soil is influenced by the pyrolyzed material. Biochars from plant biomass contain fewer nutrients than biochars from animal products. This would also be confirmed by the conclusions from the pot experiment, where higher average fruit weights were observed on variants with biochar from sewage sludge compared to sludge from wood biomass.

6.2.2 Effect of PFAS on fruit weight

Conversely, the application of contaminants to plants could lead to a decrease in fruit yield compared to variants treated only with tap water. In the case of the pot experiment, however, the yields of plants grown on the variants treated with PFAS were higher than the variants with biochar and treated with tap water.

The negative effects of PFAS on plant growth are described in their work by Li et al. (2022). An excessive amount of PFAS in plants leads to the formation of reactive oxygen radicals, which can further damage the functions of plant organelles and entire plant cells. At the same time, they can disrupt selected biochemical processes such as photosynthesis, protein synthesis, or nitrogen and carbon metabolism. This can lead to a change in the permeability of cell membranes, chlorophyll content or seed germination, root elongation or growth rate and the final size of the plant itself can be affected. Changes caused by an increased amount of reactive oxygen radicals have already been observed in some plants (wheat, lettuce, red chicory), but at the molecular level.

Growth inhibition and physiological changes in plants due to PFAS would only occur at concentrations exceeding by several orders of magnitude the normally determined concentration in plants. According to Li et al. (2022) the normal concentrations in plants are in the range of ng - µg/g. A similar range was confirmed in the work by Ghisi et al. (2019), who investigated the concentration of PFAS (including PFOA and PFOS) in cucumbers (family Cucurbitaceae, i.e. the same as zucchini and therefore similarity between these types of vegetables can be expected) grown on contaminated soils (PFAS concentration: 0.406mg/kg; 0.805 mg/kg), further enriched with sewage sludge containing PFOA and PFOS. Here, too, the average concentration of contaminants in plant tissues ranged from units to tens of ng/g of fresh matter or from units to hundreds of ng/g of dry matter. A higher concentration of PFOA (23.8 ng/g fresh matter) and PFOS (1.3 ng/g fresh matter) was measured in the soil with a higher initial concentration of PFAS. In the soil with a lower initial concentration, the measured concentration of PFOA was 11.3 ng/g fresh matter, PFOS was not detected in the plant. The concentration of PFAS in plants grown near fluorochemical industrial plants was investigated in the work of Wang et al. (2020a). Even here, concentrations exceeding hundreds of ng PFAS/g of plants were not recorded. Specifically, a concentration of 87 ng PFAS/g fresh biomass was measured in vegetables, a concentration of 480 ng/g dry matter in wheat grains, and 59 ng/g dry matter in corn grains. Even near a PFAS source, PFAS concentrations in plant tissues should not rise to such a value that changes in plant physiology can be observed.

The PFAS concentration values also in the pot experiment ranged from tenths to tens of ng PFAS/g of dry matter or hundredths to units of ng PFAS/g of fresh matter. Therefore, it cannot be assumed that the amount of PFAS would negatively affect the growth of the plant. On the contrary, a higher yield was observed in plants. The reason may be an effect called hormesis, where a contaminant that is toxic in larger doses strengthens the defense system of plants in small doses and stimulates their growth and reproduction. The hormesis effect has been described for contaminants such as pharmaceuticals, heavy metals, pesticides, microplastics, nanomaterials, flame retardants, and rare earth elements (Agathokleous et al. 2023). It is therefore possible to assume that the hormesis effect will occur even after the application of PFAS.

6.3 Effect of biochar on PFAS uptake

6.3.1 Uptake of PFAS by plants

Of the applied PFAS (HFPO-DA, HFPO-TA, HFPO-TeA, PFOA, PFOS), the contaminants HFPO-DA, PFOA, and PFOS were taken up by plants to a certain extent. HFPO-TA was detected across all variants in the order of tenths to tens ng/pot but not in all plants. The reason for the reduced uptake of this contaminant may be the higher molecular weight (496 g/mol) (Renyet et al. 2023) compared to HFPO-DA and PFOA or the higher molecular branching compared to PFOS. HFPO-TeA was detected in only 2 plants in the PFAS SSBC variant in the order of tenths to units of ng/pot. The reason for the low to zero uptake of this contaminant may be the high molecular weight (662 g/mol) caused by the longer chain of the HFPO-TeA molecule.

Plant physiology may also play a role in the limited uptake of these larger PFAS molecules. In the roots of plants from the Cucurbitaceae family, there is a Casparian strip (Fujita & Inui 2021), which limits the transport of larger PFAS molecules further into the plants (Wang et al. 2020a). Larger PFAS molecules could therefore be retained not only in the soil but also in the root. However, the roots were not examined in this work, so it cannot be determined exactly whether HFPO-TA and HFPO-TeA reached to a greater extent in other parts of the plants.

On the contrary, HFPO-DA was the compound found at the highest amount in zucchini fruits among other tested PFAS. The reason for the high uptake (in the order of tens to hundreds of ng/pot) of HFPO-DA may be the shortness and branching of the molecular chain. The higher uptake of PFAS with a short and branched chain was pointed out in the work by Mei et al. (2021) and Xu et al. (2022). Another reason for the greater amount of HFPO-DA in zucchini fruits may be the higher mobility of HFPO-DA in the soil environment. The higher mobility of GenX (HFPO-DA) caused by a lower affinity to soil compared to longer PFOA, was pointed out in the work by Liu et al. (2023).

PFOA and PFOS also accumulated in the zucchini fruits. From the graphs in Figures 17 and 18, it can be seen that PFOA accumulated more in the fruits compared to PFOS. The higher accumulation of PFCA compared to PFSA was pointed out in the work by Wang et al. (2020a). The reason for the higher accumulation of PFOA in plants is the smaller size of the functional group and the higher solubility of the molecule compared to PFOS. A higher concentration of PFOA in plants compared to PFOS was also recorded in the works of Ghisi et al. (2019), Colomer-Vidal et al. (2022), and Wang et al. (2020a).

For the last 3 named contaminants, i.e. HFPO-DA, PFOA, and PFOS, a statistically significant dependence between the amount of contaminant and fruit weight was observed. Thus, larger fruits accumulated more HFPO-DA, PFOA, and PFOS than smaller fruits. The reason for the higher accumulation of PFAS may be a higher amount of water in larger fruits, and therefore a higher amount of contaminants, as they are contained in the water. However, it cannot be reliably determined whether the heavier fruits were older than the lighter ones.

6.3.2 Effect of biochar on PFAS uptake

The application of biochars to soil did not cause a statistically significant reduction in plant uptake of PFAS, although biochars are considered materials capable of sorbing inorganic and organic contaminants, including PFAS, in soil (Yaashikaa et al. 2020). In the case of HFPO-TA, PFOA, and PFOS, a greater amount of contaminant per pot was even detected in the variants with applied biochar compared to the PFAS variant without biochar. For HFPO-DA, the amount of contaminant was higher for the PFAS WBC variant compared to the PFAS variant, for HFPO-TeA the contaminant was recorded in only 2 plants on the PFAS SSBC variant. The reasons for reduced PFAS biochar sorption are not entirely clear. Both biochars were produced at a temperature of 600 °C, which is considered to be the limit for the formation of a high sorption surface. At the same time, these biochars were applied to soil with low TOC (1.4%). For such soils, Askeland et al. (2020) and Sørmo et al. (2021) observed a 90% reduction in PFAS leaching at an application dose of 0.5% biochar to the soil (the same dose as in the pot experiment). Worse sorption capabilities of biochar were observed in soils with high TOC, which were not used in the pot experiment. A possible explanation for the reduced sorption capacity of biochar is the difference between the input pyrolyzed material and the pyrolysis process itself. Brtnický et al. (2021) drew attention to changes in sorption even with a slight change in input parameters.

When comparing the efficiency between biochars, it can be seen that plants grown on the PFAS SSBC variant contained higher amounts of HFPO-TA, HFPO-TeA, and PFOS, while plants grown on the PFAS WBC variant contained higher amounts of HFPO-DA and PFOA.

Krahn et al. (2023) observed a greater number of pores in a size suitable for PFCA sorption in sewage sludge biochar. In the pot experiment, sludge biochar sorbed better the shorter PFCA representatives, i.e. HFPO-DA and PFOA compared to the longer PFCA representatives, i.e. HFPO-TA and HFPO-TeA. The reason for the different sorption may be the pore size, which was no longer sufficient for the larger PFAS molecules, and they therefore could not be properly sorbed. For wood biochar, Askeland et al. (2020) and Sørmo et al. (2021) observed higher sorption of PFSA compared to PFCA. This trend was also observed in the pot experiment. The average amount of PFOS in fruits was lower in plants grown on the PFAS WBC variant compared to the PFAS SSBC. At the same time, a reduced ability to sorb short-chain PFAS, represented in this experiment by HFPO-DA, was observed for both biochars. The reduced sorption capacity of short PFAS by biochar from wood and sewage sludge was described in the work of Sørmo et al. (2021) and Krahn et al. (2023).

6.4 The riskiness of fruits when consumed

6.4.1 Riskiness of fruits for adults

The assessment of the risk of consuming contaminated fruit was based on the values of PFAS concentrations in fresh matter (Table 9). These values were compared with the acceptable value of the weekly intake of the amount of PFAS (determined for PFOA, PFOS, PFNA, and PFHxS, here the last two mentioned were replaced by HFPO-DA, HFPO-TA, and HFPO-TeA, for which limits have not yet been set in food), which it is 4.4 ng/kg body weight (Kule et al. 2021). For an 80 kg adult, consuming more than 352 ng PFAS/week would be a problem. It

was determined that an average adult weighing 80 kg can eat 600-800 g of zucchini per week during the season (the average weight of zucchini is around 300 g, and the zucchini grown during the experiment weighed on an average of around 200 g), off-season around 300 g of zucchini/week, but also less.

First, the riskiness of the fruits will be assessed when contaminated with only one contaminant. When comparing the specified parameters with the average concentrations of specific PFAS in fresh matter, it is evident that zucchini containing HFPO-DA contaminants, grown on PFAS and PFAS WBC variants, would appear problematic in the case of consumption of 1 fruit per week. In the case of zucchini grown on the PFAS variant, the limit of 352 ng/week would be exceeded by consuming 233 g of the fruit. For zucchini grown on the PFAS WBC variant, the weekly limit for PFAS would already be exceeded by consuming 188 g of the fruit.

But if the dose of zucchini consumed increased to 600-800 g, i.e. about 3 fruits per week, HFPO-DA-containing fruits that were grown on the PFAS SSBC variant and PFOA-containing fruits that were grown on all variants would also pose a risk. In the case of the HFPO-DA contaminant (PFAS SSBC variant), the limit of 352 ng PFAS/week would be exceeded by consuming 457 g of zucchini. In the case of the PFOA contaminant, the measured concentrations in fresh biomass were lower, therefore the amount of zucchini consumed needed to exceed the weekly limit for PFAS consumption would be higher. In the case of zucchini grown on the PFAS variant, to exceed the limit of 352 ng PFOA/week, it would be necessary to consume at least 782 g of zucchini. For the PFAS WBC variant, it would be necessary to consume 677 g of zucchini. For the PFAS SSBC variant, to exceed the limit, it would be necessary to consume at least 1136 g of zucchini, i.e. almost 4 zucchini (in the case of an average weight of 300 g). For the other contaminants, the measured concentrations in fresh biomass were so low (HFPO-TA in all variants, PFOS in all variants, HFPO-TeA in the SSBC variant), or none (HFPO-TeA in the PFAS and PFAS WBC variants) that the risk would be consumption exceeding several dozen pieces of zucchini (average weight 300 g) per week or consumption would not pose a risk. Consumption of fruits containing PFOS would be risky after exceeding the amount in the range of 20-30 pieces of zucchini per week, fruits containing HFPO-TA would be risky when consuming 58 or more fruits, in the PFAS variant even more than 117 fruits per week. Fruits containing HFPO-TeA (the PFAS SSBC variant) would be as risky as fruits containing HFPO-TA (the PFAS variant), i.e. when consuming more than 117 fruits per week.

From the previous data, it is clear that the consumption of fruits containing only 1 contaminant (HFPO-DA, PFOA) would be problematic. However, in this experiment, the plants were exposed to a mixture of contaminants, so the potential risk of fruits containing 2 contaminants (PFOA and PFOS, for which limits are set) and all 5 contaminants (HFPO-DA, HFPO-TA, HFPO-TeA, PFOS, and PFOA) will be discussed. When assessing the risk of fruits containing PFOA and PFOS contaminants, consumption of 2.3 zucchini (704 g) per week for the PFAS variant, 3.4 zucchini (1006 g) per week for the PFAS SSBC variant, and 2.1 zucchini (618 g) per week for the PFAS WBC variant would be considered problematic. If zucchini fruits were contaminated with all the selected contaminants, there would be a risk of consuming already 174 g of zucchini grown on the PFAS variant, 306 g of zucchini grown on the PFAS variant SSBC, and only 143 g of zucchini grown on the PFAS variant WBC per week. In reality, however, the contaminants HFPO-DA, PFOA, and PFOS contributed to the contamination of

fruits with PFAS, the contaminants HFPO-TA and HFPO-TeA were contained in zucchini fruits in very low concentrations.

6.4.2 Riskiness of fruits for children

If the model consumer of contaminated zucchini was a child weighing 20 kg, the limit dose for him would be 88 ng PFAS/week. A child was calculated to consume 1 zucchini per week, i.e. roughly 200 to 300 g. As with adults, the consumption of fruits containing the contaminant HFPO-DA or PFOA would be risky for children. For both contaminants, the weekly PFAS limit would be exceeded by consuming less than 300 g of zucchini. In the case of the HFPO-DA contaminant, the weekly limit for the PFAS variant would be exceeded by consuming more than 58 g of zucchini, for the PFAS SSB variant, the limit would be exceeded by consuming more than 114 g of the fruit, and for the PFAS WBC variant, the limit would be exceeded by consuming more than 47 g zucchini. For PFOA, the weekly limit for consumption would be exceeded by consuming 195 g of zucchini grown on the PFAS variant, by consuming 284 g of zucchini grown on the PFAS variant SSBC, or by consuming 169 g of zucchini grown on the PFAS variant WBC.

Fruits containing a sum of 2 (PFOA, PFOS) and 5 contaminants (HFPO-DA, HFPO-TA, HFPO-TeA, PFOS, and PFOA) would pose a risk to a 20 kg child. If a child were to consume fruit containing the sum of 2 contaminants, the weekly consumption limit would be exceeded when consuming 176 g of fruit for the PFAS variant, 251 g of fruit for the PFAS SSBC variant, and 154 g of fruit for the PFAS WBC variant. If the zucchini fruit contained the sum of all 5 PFAS, the weekly limit for consumption would be exceeded by consuming 43 g of zucchini grown on the PFAS variant, 77 g of zucchini grown on the PFAS variant SSBC, and 36 g of zucchini grown on the PFAS variant WBC. In all cases, it would therefore be problematic for a child to consume even one zucchini (in the case of contamination with all selected PFAS, even just part of the fruit), as the weekly limit for PFAS in food would be exceeded.

If the plants were irrigated with water containing PFAS, which Xu et al. (2021) described in their work, the concentration of PFAS (specifically PFOA and PFOS) in water would range from tenths to thousands of ng/L. Therefore, it is possible to assume that zucchini fruits treated with solutions with the same concentration as that presented in the work of Xu et al. (2021) contained 10 to 100,000 less PFAS than zucchini fruits in the pot experiment. To exceed the limit doses for consumption, an 80 kg adult or a 20 kg child would have to eat 10 times to 100,000 times the weight of zucchini than was calculated for the pot experiment. A 10-fold increase in the weight of consumed zucchini would still represent a real consumed dose in some variants (zucchini containing the sum of all contaminants grown on all variants), but a dose increased by 100 times or more would no longer be realistically consumable.

If zucchini plants were irrigated with a GenX solution of the concentration reported by Gebbin & van Leeuwen (2020) in the case of water from the Rhine or Nieuwe Waterweg or in the groundwater around the city of Dordrecht, the concentration would be 100 to 100,000 times lower than in pot experiment. It can therefore be assumed that zucchini watered with this water would not pose a risk when consuming 1-3 fruits in an adult and 1 fruit in a child per week, as the amount of HFPO-DA received would be 2-5 orders of magnitude lower than in the pot experiment, and therefore there would be no to exceed the limit for PFAS consumption per

week. In contrast, the concentration of GenX in the water flowing from the Dordrecht sewage treatment plant or the concentration of PFAS in the Ohio River was 10 times higher (Hopkins et al. 2018) than the concentration in the pot experiment. It would therefore be risky to consume tens of grams of zucchini per week for an adult and units of grams of zucchini per week for a child.

7 Conclusion

- Zucchini plants (*Cucurbita pepo* L.) were irrigated with a PFAS solution (HFPO-DA, HFPO-TA, HFPO-TeA, PFOA, PFOS) or a control solution (methanol) in the pot experiment.
- The concentration of PFAS in the solution (10 µg/L) was chosen based on data from scientific literature. However, such concentration values in water have not yet been detected in the Czech Republic.
- Biochar made from sewage sludge and waste wood was used as a remediation agent for removing PFAS from irrigation water.
- No statistically significant increase in fruit biomass production was observed after the application of biochar, although biochar is considered a material that improves soil quality and crop yield. On the contrary, the graphs showed a slight decrease in the increase in biomass. The reason could be the sorption of important nutrients on the surface of the biochar, which the plants subsequently lacked during growth.
- No statistically significant decrease in the increase in fruit biomass was observed between the variants watered with the PFAS solution and the control solution. From the graphs, on the other hand, a slight increase in fruit biomass was recorded for plants watered with a PFAS solution compared to plants watered with a methanol solution. The reason may be an effect called hormesis.
- In plants with applied biochar, no statistically significant difference in PFAS uptake was recorded compared to the control variant. Contaminants were recorded in variants with and without biochar. In the case of HFPO-TA, PFOA, and PFOS, a larger amount of contaminant per pot was even detected in the variants with applied biochar compared to the PFAS variant without biochar.
- Contaminants HFPO-TA, HFPO-TeA, and PFOS were more taken up by plants grown on the PFAS variant SSBC. More PFOA and HFPO-DA were recorded in plants grown on WBC variants.
- HFPO-TeA and HFPO-TA were the least detected in plants in all variants. The reason could be the high molecular weight of the given contaminants or the length of the carbon chain. On the contrary, HFPO-DA was the most uptake by plants in all variants. The reason could be the branching of the chain or the high mobility of HFPO-DA in the soil environment.
- PFOA accumulated more in fruits than PFOS. The reason could be the smaller size of the functional group of PFOA and the higher solubility of PFOA compared to PFOS.
- The risk dose for an adult person (80 kg) is 352 ng PFAS/week. This dose would be achieved by consuming 143 to 306 g of zucchini, depending on the variant. For a child (20 kg), the risk intake is 88 ng PFAS/week. This dose would be achieved by consuming 36 to 77 g of zucchini, depending on the variant. In both cases, this is a dose that the given person can consume weekly without any problems.

8 Bibliography

- Agathokleous E, Liu ChJ, Calabrese EJ. 2023. Applications of the hormesis concept in soil and environmental health research. *Soil & Environmental Health*. **1**: 100003.
- Agency for Toxic Substances and Disease Registry. 2022. What are PFAS? Agency for Toxic Substances and Disease Registry, Spain. Available from <https://www.atsdr.cdc.gov/pfas/health-effects/overview.html> (Accessed October 2023).
- American Water Works Association. 2019. Per- and Polyfluoroalkyl Substances (PFAS) Overview and Prevalence. American Water Works Association. Available from [https://www.awwa.org/Portals/0/AWWA/ETS/Resources/Per-andPolyfluoroalkylSubstances\(PFAS\)-OverviewandPrevalence.pdf?ver=2019-08-14-090234-873](https://www.awwa.org/Portals/0/AWWA/ETS/Resources/Per-andPolyfluoroalkylSubstances(PFAS)-OverviewandPrevalence.pdf?ver=2019-08-14-090234-873) (Accessed October 2023).
- Askeland M, Clarke BO, Cheema SA, Mendez A, Gasco G, Paz-Ferreiro J. 2020. Biochar sorption of PFOS, PFOA, PFHxS, and PFHxA in two soils with contrasting textures. *Chemosphere*. **249**: 126072.
- Bao Y, Qu Y, Huang J, Cagnetta G, Yu G, Weber R. 2017. First assessment on the degradability of sodium p-perfluorooctane sulfonate (OBS), a high-volume alternative to perfluorooctane sulfonate in fire-fighting foams and oil production agents in China. *RSC Advances*. **7**: 46948–46957.
- Brandsma SH, Koekkoek JC, van Velzen MJM, de Boer J. 2019. The PFOA substitute GenX detected in the environment near a fluoropolymer manufacturing plant in the Netherlands. *Chemosphere*. **220**: 493-500.
- Brtnický M, Fatta R, Holatko J, Bielska L, Gusiati ZM, Kucerik J, Hammerschmidt T, Danish S, Radziemska M, Mravcova L, Fahad S, Kintl A, Sudoma M, Ahmed N, Pecina V. 2021. A critical review of the possible adverse effects of biochar in the soil environment. *Science of The Total Environment*. **796**: 148756.
- Buck RC, Franklin J, Berger U, Conder JM, Cousins IT, Voogt P, Jensen AA, Kannan K, Mabury SA, Leeuwen SPJ. 2011. Perfluoroalkyl and Polyfluoroalkyl Substances in the Environment: Terminology, Classification, and Origins. *Integrated Environmental Assessment and Management*. **7**: 513-41.
- Colomer-Vidal P, Jiang L, Mei W, Luo Ch, Lacorte S, Rigol A, Zhang G. 2022. Plant uptake of perfluoroalkyl substances in freshwater environments (Dongzhulong and Xiaoqing Rivers, China). *Journal of Hazardous Material*. **421**: 126768.
- Conley J, Lambright C, Evans N, Medlock K, Kakaley E, Wilson V, Gray L. 2019. Developmental toxicity of perfluoroalkyl ether acids following oral gestational exposure: Comparison of Gen X, Nafion byproduct 2, and Perfluoro-2-methoxyacetic acid. Society of Environmental Toxicology and Chemistry, Toronto, Ontario, Canada. Available from https://cfpub.epa.gov/si/si_public_record_Report.cfm?dirEntryId=350077&Lab=CPHEA (Accessed November 2023).

- Contaminated Site Clean-Up Information (CLU-IN). 2023. Per- and Polyfluoroalkyl Substances (PFAS): Chemistry and Behavior. CLU-IN. Available from [https://clu-in.org/contaminantfocus/default.focus/sec/Per-and_Polyfluoroalkyl_Substances_\(PFAS\)/cat/Chemistry_and_Behavior/](https://clu-in.org/contaminantfocus/default.focus/sec/Per-and_Polyfluoroalkyl_Substances_(PFAS)/cat/Chemistry_and_Behavior/) (Accessed October 2023).
- Cousins IT, DeWitt JC, Glüge J, Goldenman G, Herzke D, Lohmann R, Miller M, Ng CA, Scheringer M, Vierke L, Wnag Z. 2020. Strategies for grouping per- and polyfluoroalkyl substances (PFAS) to protect human and environmental health. *Environmental Science: Processes & Impacts*. **22**: 1444-1460.
- Dong Q, Guo Y, Yuan J, Zhong S, I H, Liu J, Zhang M, Sun J, Yuan S, Yu H, Zhong Y, Jiang Q. 2023. Hexafluoropropylene oxide tetramer acid (HFPO-TeA)-induced developmental toxicities in chicken embryo: Peroxisome proliferator-activated receptor Alpha (PPAR α) is involved. *Ecotoxicology and Environmental Safety*. **253**: 114671.
- Dvorakova D, Jurikova M, Svobodova V, Parizek O, Kozisek F, Kotal F, Jeligova H, Mayerova L, Pulkrabova J. 2023. Complex monitoring of perfluoroalkyl substances (PFAS) from tap drinking water in the Czech Republic. **247**: 120764.
- Environmental Agency. 2023. Environmental risk evaluation reports: Perfluoro(2-ethoxy-2-fluoroethoxy)-acetic acid, ammonium salt [EEA-NH₄] (CAS No. 908020-52-0). Environmental Agency, Bristol. Available from https://assets.publishing.service.gov.uk/media/6421a7aefe97a8001379ecf7/8_Environmental_risk_evaluation_report_Perfluoro_2-ethoxy-2-fluoroethoxy_-_acetic_acid_ammonium_salt.pdf (Accessed February 2024).
- Fabregat-Palau J, Vidal M, Rigol M. 2021. Modeling the sorption behavior of perfluoroalkyl carboxylates and perfluoroalkane sulfonates in soils. *Science of The Total Environment*. **801**: 149343.
- Farhangi-Abriz S, Torabian S, Qui R, Noulas Ch, Lu Y, Gao S. 2021. Biochar effects on yield of cereal and legume crops using meta-analysis. *Science of The Total Environment*. **775**: 145869.
- Farid MI, Siam HS, Abbas MHH, Mohamed I, Mahmoud SA, Tolba M, Abbas HH, Yang X, Antoniadis V, Rinklebe J, Shaheen SM. 2022. Co-composted biochar derived from rice straw and sugarcane bagasse improved soil properties, carbon balance, and zucchini growth in a sandy soil: A trial for enhancing the health of low fertile arid soils. *Chemosphere*. **292**: 133389.
- Fujita K, Inui H. 2021. How does the Cucurbitaceae family take up organic pollutants (POPs, PAHs, and PPCPs)?. *Reviews in Environmental Science and Bio/Technology*. **20**: 751-779.
- Gebbink WA, Van Leeuwen SPJ. 2020. Environmental contamination and human exposure to PFASs near a fluorochemical production plant: Review of historic and current PFOA and GenX contamination in the Netherlands. *Environment International*. **137**: 105583.

- Ghisi R, Vamerali T, Manzetti S. 2019. Accumulation of perfluorinated alkyl substances (PFAS) in agricultural plants: A review. *Environmental Research*. **169**: 326-341.
- Gui W, Guo H, Chen X, Wang J, Guo Y, Zhang H, Zhou X, Zhao Y, Dai J. 2023. Emerging polyfluorinated compound Nafion by-product 2 disturbs intestinal homeostasis in zebrafish (*Danio rerio*). *Ecotoxicology and Environmental Safety*. **249**: 114368.
- Hagemann N, Schmidt HS, Kägi R, Böhler M, Sigmund G, Maccagnan A, McArdell ChS, Bucheli TD. Wood-based activated biochar to eliminate organic micropollutants from biologically treated wastewater. *Science of The Total Environment*. **730**: 138417.
- He Y, Ly D, Li Ch, Liu X, Liu W, Han W. 2022. Human exposure for F-53B in China and the evaluation of its potential toxicity: An overview. *Environmental International*. **161**: 107108.
- Henry BJ, Carlin JP, Hammerschmidt JA, Buck RC, Buxton LW, Fiedler H, Seed J, Hernandez O. 2018. A critical review of the application of polymer of low concern and regulatory criteria to fluoropolymers. *Integrated Environmental Assessment and Management*. **14**: 316-334.
- Hopkins ZR, Sun M, DeWitt JC, Knappe DRU. 2018. Recently Detected Drinking Water Contaminants: GenX and Other Per- and Polyfluoroalkyl Ether Acids. *JournalAWWA*. **7**: 13-28.
- Hu Y, Gholizadeh M. 2019. Biomass pyrolysis: A review of the process development and challenges from initial researches up to the commercialization stage. *Journal of Energy Chemistry*. **39**: 109-143.
- Huang J, Sun L, Mennigen JA, Liu Y, Liu S, Zhang M, Wang Q, Tu W. 2021. Developmental toxicity of the novel PFOS alternatives OBS in developing zebrafish: An emphasis on cilia disruption. *Journal of Hazardous Materials*. **409**: 124491.
- Huang Y, Lu M, Li H, Bai M, Huang X. 2019. Sensitive determination of perfluoroalkane sulfonamides in water and urine samples by multiple monolithic fiber solid-phase microextraction and liquid chromatography-tandem mass spectrophotometry. *Talanta*. **192**: 24-31.
- Hušková R, Vojtěchovská Šrámková M. 2021. Per- a polyfluorované alkylové sloučeniny (PFAS) v pitné vodě. Sdružení oboru vodovodů a kanalizací ČR. Available from <https://www.sovak.cz/cs/clanek/polyfluorovane-alkylove-slouceniny-pfas-v-pitne-vode> (Accessed February 2024).
- Interstate Technology & Regulatory Council (ITRC). 2023. PFAS – Per- and Polyfluoroalkyl Substances: 2.2 Chemistry, Terminology, and Acronyms. Interstate Technology and Regulatory Council, Washington D.C., USA. Available from <https://pfas-1.itrcweb.org/2-2-chemistry-terminology-and-acronyms/> (Accessed October 2023).
- Jin H, Shan G, Zhu L, Sun H, Luo Y. 2018. Perfluoroalkyl Acids Including Isomers in Tree Barks from a Chinese Fluorochemical Manufacturing Park: Implication for Airborne Transportation. *Environmental Science & Technology*. **52(4)**:2016-2024.

- Kancharla S, Choudhary A, Davis RT, Dong D, Bedrov D, Tsianou M, Alexandridis P. 2022. GenX in water: Interactions and self-assembly. *Journal of Hazardous Materials*. **428**: 128137.
- Kissa E. 2001. *Fluorinated Surfactants and Repellents, Second Edition Revised and Expanded*. Surfactant Science Series, New York.
- Krahn KM, Cornelissen G, Castro G, ARP HPH, Asimakopoulos AG, Wolf R, Holmstad R, Zimmerman AR, Sørmo E. 2023. Sewage sludge biochars as effective PFAS-sorbents. *Journal of Hazardous Materials*. **445**: 130449.
- Kule L, Sikorová L, Koželuh M. 2021. PFAS kolem nás. Sledování perfluorovaných látek (PFAS) ve vodách povodí Vltavy. Available from <https://vodnihospodarstvi.cz/pfas-kolem-nas-sledovani-perfluorovanych-latek-pfas-ve-vodach-povodi-vltavy/> (Accessed February 2024).
- Kuzniewski S. 2022. What are Per- and Polyfluoroalkyl Substances (PFAS)? Wastewater digest. Available from <https://www.wwdmag.com/what-is-articles/article/10940589/what-are-per-and-polyfluoroalkyl-substances-pfas> (Accessed October 2023).
- Lesmeister L, Lang FT, Breuer J, Biegel-Engler A, Giese E, Scheurer M. 2021. Extending the knowledge about PFAS bioaccumulation factors for agricultural plants – A review. *Science of The Total Environment*. **766**: 14640.
- Leung SCHE, Wanninayake D, Chen D, Nguyen NT, Li Q. 2023. Physicochemical properties and interactions of perfluoroalkyl substances (PFAS) - Challenges and opportunities in sensing and remediation. *Science of The Total Environment*. **905**: 166764.
- Li F, Fang Y, Zhou Z, Liao Y, Zou J, Yuan B, Sun W. 2019. Adsorption of perfluorinated acids onto soils: Kinetics, isotherms, and influences of soil properties. *Science of The Total Environment*. **649**: 504-514.
- Li J, Sun J, Li P. 2022. Exposure routes, bioaccumulation and toxic effects of per- and polyfluoroalkyl substances (PFASs) on plants: A critical review. *Environmental International*. **158**: 106891.
- Liu G, Usman M, Luo T, Biard PF, Lin K, Greenwell HCh, Hanna K. 2023. Retention and transport of PFOA and its fluorinated substitute, GenX, through water-saturated soil columns. *Environmental Pollution*. **337**: 122530.
- Liu J, Mejia Avendaño S. 2013. Microbial degradation of polyfluoroalkyl chemicals in the environment: A review. *Environment International*. **61** (2013): 98-114.
- Liu S, Yang R, Yin N, Faiola F. 2020. The short-chain perfluorinated compounds PFBS? PFHxS, PFBA and PFHxA, disrupt human mesenchymal stem cell self-renewal and adipogenic differentiation. *Journal of Environmental Sciences*. **88**: 187-199.
- Lohmann R, Letcher RJ. 2023. The universe of fluorinated polymers and polymeric substances and potential environmental impacts and concerns. *Current Opinion in Green and Sustainable Chemistry*. **41**: 100795.

- McCord J, Newton S, Strynar M. 2018. Validation of quantitative measurements and semi-quantitative estimates of emerging perfluoroethercarboxylic acids (PFECAs) and hexafluoropropylene oxide acids (HFPOAs). *Journal of Chromatography A*. **1551**: 52-58.
- Mei W, Sun H, Song M, Jiang L, Li Y, Lu W, Ying G-G, Luo Ch, Zhang G. 2021. Per- and polyfluoroalkyl substances (PFASs) in the soil-plant system: Sorption, root uptake and translocation. *Environmental International*. **156**: 106642.
- Mercl F, Tejnecký V, Száková J, Tlustoš P. 2016. Nutrient Dynamics in Soil Solution and Wheat Response after Biomass Ash Amendments. *Agronomy Journal*. **108**: 2222-2234.
- Ministerstvo životního prostředí (MŽP). 2023. Kyselina perfluorhexansulfonová (PFHxS) a její varianta mají být zakázané, vláda dnes přijala změnu mezinárodní úmluvy. Ministerstvo životního prostředí. Available from https://www.mzp.cz/cz/stockholmska_umluva_polutantny (Accessed October 2023).
- Munoz G, Liu J, Duy SV, Sauvé S. 2019. Analysis of F-53B, Gen-X, ADONA and emerging fluoroalkyl ether substances in environmental and biomonitoring samples: A review. *Trends in Environmental Analytical Chemistry*. **23**: e00066.
- Ochecova P, Tlustos P, Szakova J, Mercl F, Maciak M. 2016. Changes in Nutrient Plant Availability in Loam and Sandy Clay Loam Soils after Wood Fly and Bottom Ash Amendment. *Agronomy Journal*. **108**: 1-11.
- OECD. 2021. Reconciling Terminology of the Universe of Per- and Polyfluoroalkyl Substances: Recommendations and Practical Guidance, OECD Series on Risk Management, No. 61. OECD Publishing, Paris.
- OECD. Not dated. Portal on Per and Poly Fluorinated Chemicals: What are PFASS and what are they used for? OECD, Paris, France. Available from <https://www.oecd.org/chemicalsafety/portal-perfluorinated-chemicals/aboutpfass/> (Accessed November 2023).
- Pereira HC, Ullberg M, Berggren Kleja D, Gustafsson JP, Ahrens L. 2018. Sorption of perfluoroalkyl substances (PFASs) to an organic soil horizon – Effect of cation composition and pH. *Chemosphere*. **207**: 183-191.
- Ramírez Carneo A, Lestido Cardama A, Vázquez Loureiro P, Barbosa Pereira L, Rodríguez Bernaldo de Quirós AI, Sendón R. 2021. Presence of Perfluoroalkyl and Polyfluoroalkyl Substances (PFAS) In Food Contact Materials (FCM) and Its Migration to Food. *Foods: A review*. **2021**: 10, 1443.
- Reade A. 2018. NRDC: EPA Finds Replacements for Toxic “Teflon” Chemicals Toxic. NRDC. Available from <https://www.nrdc.org/bio/anna-reade/epa-finds-replacements-toxic-teflon-chemicals-toxic> (Accessed October 2023).
- Renyer A, Ravindra K, Wetmore BA, Ford JL, DeVito M, Hughes MF, Wehmas LC, MacMillan DK. 2023. Dose Response, Dosimetric, and Metabolic Evaluations of Replacement PFAS Perfluoro-(2,5,8-trimethyl-3,6,9-trioxadodecanoic) Acid (HFPO-TeA). *Toxics*. **11**: 951.

- Salvidge R, Hosea L. 2023. Revealed: scale of ‘forever chemical’ pollution across UK and Europe. The Guardian. Available from <https://www.theguardian.com/environment/2023/feb/23/revealed-scale-of-forever-chemical-pollution-across-uk-and-europe> (Accessed from April 2024).
- Semerád J, Hatasová N, Grasserová A, Černá T, Filipová A, Hanč A, Innemanová P, Pivokonský M, Cajthaml T. 2020. Screening for 32 per- and polyfluoroalkyl substances (PFAS) including GenX in sludges from 43 WWTPs located in the Czech Republic - Evaluation of potential accumulation in vegetables after application of biosolids. *Chemosphere*. **261**: 128018.
- Sørmo E, Silvani L, Bjerkli N, Hagemann N, Zimmerman AR, Hale SE, Hansen, CB, Hartnik T, Cornelissen G. 2021. Stabilization of PFAS-contaminates soil with activated biochar. *Science of The Total Environment*. **736**: 144034.
- Sun S, Li X, Zhang L, Zhong Z, Chen Ch, Zuo Y, Chen Y, Hu H, Liu F, Xiong G, Lu H, Chen J, Dai J. 2023. Hexafluoropropylene oxide trimer acid (HFPO-TA) disturbs embryonic liver and biliary system development in zebrafish. *Science of The Total Environment*. **859**: 160087.
- Thoma ED, Wright RS, George I, Krause M, Presezzi D, Villa V, Preston W, Deshmukh P, Kauppi P, Zemek PG. 2022. Pyrolysis processing of PFAS-impacted biosolids, a pilot study. *Journal of the Air & Waste Management Association*. **72**: 309-318.
- United States Environment Protection Agency (EPA). 2023b. Drinking Water Health Advisories for GenX Chemicals and PFBA: 2022 Final Health Advisories for GenX Chemicals and PFBS. EPA, USA. Available from <https://www.epa.gov/sdwa/drinking-water-health-advisories-genx-chemicals-and-pfbs> (Accessed October 2023).
- United States Environmental Protection Agency (EPA). 2023a. PFAS Explained. EPA, USA. Available from <https://www.epa.gov/pfas/pfas-explained> (Accessed October 2023).
- United States Environmental Protection Agency (EPA). 2023c. Technical fact sheet: Human Health Toxicity Assessment for GenX Chemicals. EPA, USA. Available from <https://www.epa.gov/system/files/documents/2023-03/GenX-Tox-Assessment-technical-factsheet-March-2023-Update.pdf> (Accessed February 2024).
- United States Environmental Protection Agency (EPA). 2023d. Questions and Answers: Drinking Water Health Advisories for PFOA, PFOS, GenX Chemicals, and PFBS. EPA, USA. Available from <https://www.epa.gov/sdwa/questions-and-answers-drinking-water-health-advisories-pfoa-pfos-genx-chemicals-and-pfbs> (Accessed February 2024).
- Wallace JS, Edirisinghe D, Seyedi S, Noteboom H, Blate M, Balci DD, Abu-Orf M, Sharp R, Brown J, Aga DS. 2023. Burning questions: Current practices and critical gaps in evaluating removal of per- and polyfluoroalkyl substances (PFAS) during pyrolysis treatments of biosolids. *Journal of Hazardous Materials Letters*. **4**: 100079.
- Wang TT, Ying GG, He LY, Liu YS, Zhao JL. 2020b. Uptake mechanism, subcellular distribution, and uptake process of perfluorooctanoic acid and perfluorooctane sulfonic acid by wetland plant *Alisma orientale*. *Science of The Total Environment*. **733**: 139383.

- Wang W, Rhodes G, Ge J, Yu X, Li H. 2020a. Uptake and accumulation of per- and polyfluoroalkyl substances in plants. *Chemosphere*. **261**: 127584.
- Xin, X, Ren XM, Wan B, Guo LH. 2019. Comparative in Vitro and in Vivo Evaluation of the Estrogenic Effect of Hexafluoropropylene Oxide Homologues. *Environmental Science and Technology*. **53 (14)**: 8371-8380.
- Xu B, Lio S, Zhou JK, Zheng Ch, Jin W, Chen B, Zhang T, Qiu W. 2021. PFAS and their substitutes in groundwater: Occurrence transformation and remediation. *Journal of Hazardous Materials*. **412**: 125159.
- Xu B, Qiu W, Du J, Wan Z, Zhou JL, Chen H, Liu R, Magnuson JT, Zheng Ch. 2022. Translocation, bioaccumulation, and distribution of perfluoroalkyl and polyfluoroalkyl substances (PFASs) in plants. *iScience*. **25**: 104061.
- Yasshikaa PR, Snethil Kumar P, Varjani S, Sarvanan A. 2020. A critical review of the biochar production techniques, characterization, stability, and applications for circular economy. *Biotechnology Report*. **28**: e00570.
- Zhang DQ, Wang M, He Q, Niu X, Liang Y. 2020. Distribution of perfluoroalkyl substances (PFASs) in aquatic plant-based systems: From soil adsorption and plant uptake to effects on microbial community. *Environmental Pollution*. **257**: 113575.
- Zhou L, He S, Shi Y, Cai Y, Zhang Ch. 2022. Tissue distribution of sodium p-perfluorooctanesulfonate (OPS) in mice via oral exposure. *Environment International*. **165**: 107289.

9 Appendices

9.1 Appendix 1 – Weight of zucchini fruits

variety		Fresh Weight [g]	Dry Weight [g]
control	POT 1	216.48	35.9
	POT 2	268.5	14.14
	POT 3	359.01	16.3
	POT 4	No plant	
	POT 5	245.14	14.8
control SSSBC	POT 6	80.56	5.17
	POT 7	32.8	2.77
	POT 8	238.55	13.29
	POT 9	9.58	0.83
	POT 10	283.41	15.3
control WBC	POT 11	25.4	2.13
	POT 12	26.3	2.07
	POT 13	321.63	15.22
	POT 14	57.01	3.92
	POT 15	210.27	9.24
PFAS	POT 16	27.4	2.46
	POT 17	152.43	8.51
	POT 18	338.42	16.18
	POT 19	93.02	6.27
	POT 20	238.23	15.12
PFAS SSSBC	POT 21	253.99	15.39
	POT 22	296.19	13.65
	POT 23	93.84	5.28
	POT 24	No fruit	
	POT 25	268.8	14.66
PFAS WBC	POT 26	214.69	10.71
	POT 27	41.39	3.06
	POT 28	58.3	3.79
	POT 29	192.1	9.21
	POT 30	232.37	11.89

9.2 Appendix 2 – Concentrations of contaminants measured in individual plants

		HFPO-DA	HFPO-TA	HFPO-TeA	PFOA	PFOS
		[ng/g dry biomass]				
PFAS	POT 16	25.6	0.17	0	6.49	0.64
	POT 17	36.31	0	0	13.61	1.18
	POT 18	21.98	0.14	0	7.12	0.49
	POT 19	19.05	0.21	0	4.75	0.54
	POT 20	14.11	0	0	4.2	0.8
PFAS SSBC	POT 21	25.28	0.31	0	11.42	0.85
	POT 22	22.39	0.16	0	6.47	0.86
	POT 23	0	0	0.04	0	0
	POT 24	No fruit				
	POT 25	9.79	0.57	0.58	4.63	0.84
PFAS WBC	POT 26	27.33	0.03	0	6.72	1.33
	POT 27	28.72	0	0	3.42	0.23
	POT 28	27.38	0.39	0	7.94	0.8
	POT 29	18.89	0.15	0	5.96	0.7
	POT 30	61.96	0.99	0	23.61	1.73
		[ng/g fresh biomass]				
PFAS	POT 16	2.3	0.02	0	0.58	0.06
	POT 17	2.03	0	0	0.76	0.07
	POT 18	1.05	0.01	0	0.34	0.02
	POT 19	1.28	0.01	0	0.32	0.04
	POT 20	0.9	0	0	0.27	0.05
PFAS SSBC	POT 21	1.53	0.02	0	0.69	0.05
	POT 22	1.03	0.01	0	0.3	0.04
	POT 23	0	0	0	0	0
	POT 24	No fruit				
	POT 25	0.53	0.03	0.03	0.25	0.05
PFAS WBC	POT 26	1.36	0	0	0.34	0.07
	POT 27	2.12	0	0	0.25	0.02
	POT 28	1.78	0.03	0	0.52	0.05
	POT 29	0.91	0.01	0	0.29	0.03
	POT 30	3.17	0.05	0	1.21	0.09

9.3 Appendix 3 – Amount of contaminants measured in individual plants

variety		HFPO-DA	HFPO-TA	HFPO-TeA	PFOA	PFOS
		[ng]				
PFAS	Pot 16	63.07	0.43	0	15.99	1.58
	Pot 17	309	0	0	115.81	10.01
	Pot 18	355.55	2.24	0	115.24	7.95
	Pot 19	119.39	1.31	0	29.78	3.41
	Pot 20	213.29	0	0	63.53	12.08
PFAS SSBC	Pot 21	389.1	4.79	0	175.78	13.12
	Pot 22	305.7	2.21	0	88.34	11.81
	Pot 23	0	0	0.22	0	0
	Pot 24	No fruit				
	Pot 25	143.47	8.42	8.45	67.91	12.3
PFAS WBC	Pot 26	292.64	0.27	0	71.99	14.26
	Pot 27	87.76	0	0	10.46	0.71
	Pot 28	103.85	1.48	0	30.13	3.03
	Pot 29	173.96	1.4	0	54.9	6.47
	Pot 30	736.4	11.78	0	280.66	20.59

9.4 Appendix 4 – Uptake of contaminants from individual plants

variety		Uptake of HFPO-DA	Uptake of HFPO-TA	Uptake of HFPO-TeA	Uptake of PFOA	Uptake of PFOS
		[%]				
PFAS	POT 16	0.081	0.001	0	0.02	0.002
	POT 17	0.395	0	0	0.148	0.013
	POT 18	0.455	0.003	0	0.147	0.01
	POT 19	0.153	0.002	0	0.038	0.004
	POT 20	0.273	0	0	0.081	0.015
PFAS SSBC	POT 21	0.498	0.006	0	0.225	0.017
	POT 22	0.391	0.003	0	0.113	0.015
	POT 23	0	0	0.221	0	0
	POT 24	No fruit				
	POT 25	0.184	0.011	0.011	0.087	0.016
PFAS WBC	POT 26	0.374	0	0	0.092	0.018
	POT 27	0.112	0	0	0.013	0.001
	POT 28	0.133	0.002	0	0.039	0.004
	POT 29	0.223	0.002	0	0.07	0.008
	POT 30	0.262	0.015	0	0.131	0.015